Article

Current Biology

Mitochondria-derived reactive oxygen species are the likely primary trigger of mitochondrial retrograde signaling in *Arabidopsis*

Highlights

- Mitochondria modulate nuclear gene expression through retrograde regulation (MRR)
- Many parameters linked to mitochondrial function do not directly drive MRR in plants
- Mitochondrial reactive oxygen species likely act as primary trigger to induce MRR
- Mitochondrial ROS may not need to leak into the cytosol or ER lumen to trigger MRR

Authors

Kasim Khan, Huy Cuong Tran, Berivan Mansuroglu, ..., Alex Costa, Allan G. Rasmusson, Olivier Van Aken

Correspondence

olivier.van_aken@biol.lu.se

In brief

By monitoring a wide range of mitochondrial-function-related physiological parameters and second messengers in real time, Khan et al. report that mitochondria-produced reactive oxygen species are the most likely primary trigger for mitochondria-to-nuclear "retrograde" signaling in plants.

Khan et al., 2024, Current Biology *34*, 1–16
January 22, 2024
https://doi.org/10.1016/j.cub.2023.12.005

CellPress

Please cite this article in press as: Khan et al., Mitochondria-derived reactive oxygen species are the likely primary trigger of mitochondrial retrograde signaling in *Arabidopsis*, Current Biology (2023), https://doi.org/10.1016/j.cub.2023.12.005

Current Biology

CellPress
OPEN ACCESS

Article

Mitochondria-derived reactive oxygen species are the likely primary trigger of mitochondrial retrograde signaling in *Arabidopsis*

Kasim Khan,[1] Huy Cuong Tran,[1] Berivan Mansuroglu,[1,5] Pinar Önsell,[1] Stefano Buratti,[2] Markus Schwarzländer,[3] Alex Costa,[2,4] Allan G. Rasmusson,[1] and Olivier Van Aken[1,6,*]

[1]Department of Biology, Lund University, Sölvegatan 35, Lund 223 62, Sweden
[2]Department of Biosciences, University of Milan, Via G. Celoria 26, Milan 20133, Italy
[3]Plant Energy Biology Lab, Institute of Plant Biology and Biotechnology, University of Münster, Schlossplatz 8, 48143 Münster, Germany
[4]Institute of Biophysics, Consiglio Nazionale delle Ricerche, Via G. Celoria 26, 20133 Milan, Italy
[5]Present address: Institute of Physiology I, Medical Faculty, University of Bonn, Nussallee 11, 53115 Bonn, Germany
[6]Lead contact
*Correspondence: olivier.van_aken@biol.lu.se
https://doi.org/10.1016/j.cub.2023.12.005

SUMMARY

Besides their central function in respiration, plant mitochondria play a crucial role in maintaining cellular homeostasis during stress by providing "retrograde" feedback to the nucleus. Despite the growing understanding of this signaling network, the nature of the signals that initiate mitochondrial retrograde regulation (MRR) in plants remains unknown. Here, we investigated the dynamics and causative relationship of a wide range of mitochondria-related parameters for MRR, using a combination of *Arabidopsis* fluorescent protein biosensor lines, *in vitro* assays, and genetic and pharmacological approaches. We show that previously linked physiological parameters, including changes in cytosolic ATP, NADH/NAD$^+$ ratio, cytosolic reactive oxygen species (ROS), pH, free Ca^{2+}, and mitochondrial membrane potential, may often be correlated with—but are not the primary drivers of—MRR induction in plants. However, we demonstrate that the induced production of mitochondrial ROS is the likely primary trigger for MRR induction in *Arabidopsis*. Furthermore, we demonstrate that mitochondrial ROS-mediated signaling uses the ER-localized ANAC017-pathway to induce MRR response. Finally, our data suggest that mitochondrially generated ROS can induce MRR without substantially leaking into other cellular compartments such as the cytosol or ER lumen, as previously proposed. Overall, our results offer compelling evidence that mitochondrial ROS elevation is the likely trigger of MRR.

INTRODUCTION

Mitochondria are actively engaged in feedback communication with the nucleus to maintain organellar function during stress and development.[1] This mitochondrial retrograde regulation (MRR) relays signals that originate in the mitochondria due to physiological changes to the nucleus to modulate nuclear gene expression.

Several plant MRR target genes were identified by inhibition of mitochondrial respiration by, e.g., antimycin A (AA) (complex III inhibitor) or mutants impaired in mitochondrial functions.[2] The promoter of these genes contains a *cis*-regulatory mitochondrial dysfunction motif (MDM).[3,4] Many of these mitochondrial dysfunction stimulon (MDS) genes play important roles during plant stress responses.[5–8] For instance, alternative oxidase *AOX1a* is important for stress tolerance, including osmotic stress.[9,10] *AOX1a* acts as an alternative electron acceptor, providing a safety valve for metabolic over-reduction when the cytochrome *c* oxidase pathway is inhibited.[11,12]

A group of NAC (NAM, ATAF1/2, and CUC2) transcription factors, particularly ANAC017, was identified as master mediators of MRR in *Arabidopsis*.[4,7,13] ANAC017 is anchored to the endoplasmic reticulum (ER) membrane by a C-terminal transmembrane domain.[14] During mitochondrial stress conditions, ANAC017 is cleaved by rhomboid proteases, likely in its transmembrane domain, and translocates to the nucleus to reprogram expression of MRR target genes involved in respiration and various other functions.[4,7,15]

MRR must thus be triggered by a mitochondrial signal that is relayed to the ER to trigger ANAC017 release. However, the primary signals generated during mitochondrial dysfunction are still unknown in plants. Evidence in yeast showed that decreased cellular ATP levels or energy charge during mitochondrial dysfunction could trigger MRR induction through the "retrograde" (RTG) pathway.[16–19] Disruption in mitochondrial membrane potential ($\Delta\psi_m$) by defects in mitochondrial electron transport chain (mtETC) or mitochondrial DNA was also suggested to trigger an RTG response in yeast.[20] In mammalian systems, a drop in $\Delta\psi_m$ was proposed as the main trigger of the RTG response, impairing mitochondrial Ca^{2+} uptake and increasing levels of cytosolic Ca^{2+}. This leads to the activation of ATF2, NFAT, and nuclear factor (NF)-κB to initiate the mitochondrial dysfunction response.[21–24] Additionally, the NADH/NAD$^+$ ratio and reactive oxygen species (ROS) have also been linked to retrograde responses in mammals.[25–27]

Please cite this article in press as: Khan et al., Mitochondria-derived reactive oxygen species are the likely primary trigger of mitochondrial retrograde signaling in *Arabidopsis*, Current Biology (2023), https://doi.org/10.1016/j.cub.2023.12.005

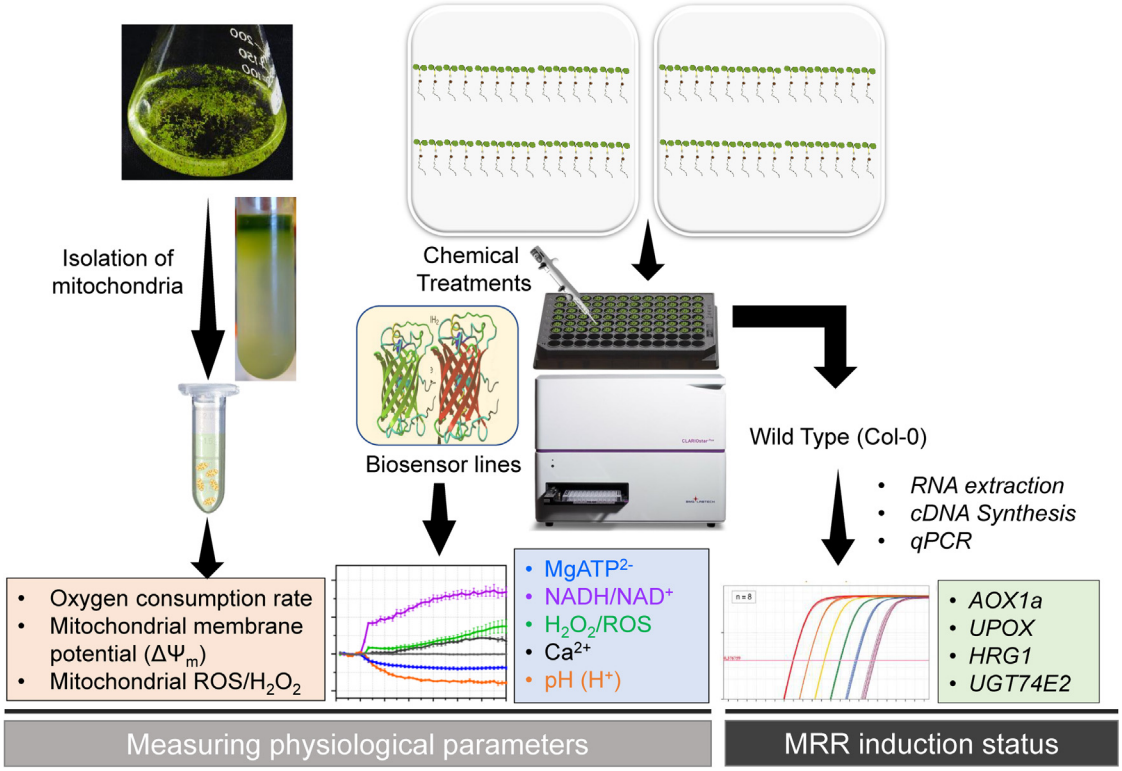

Figure 1. Schematic illustration and workflow for monitoring mitochondria-related physiological parameters and transcript analysis

7-day-old seedlings growing vertically on half-strength MS plates were used for monitoring physiological parameters. Five seedlings of genetically encoded biosensor lines and Col-0 were submerged in assay medium in 96-well plates and monitored in a multi-well plate reader. Col-0 seedlings were treated identically as the plate reader biosensor assays for gene expression analysis. Col-0 seedlings were grown in liquid half-strength MS media for mitochondrial isolation to measure mitochondrial ROS/H_2O_2, mitochondrial membrane potential ($\Delta\psi_m$), and oxygen consumption rate. The figure is related to STAR Methods. See also Tables S1 and S2.

In plants, recent studies proposed several signaling molecules as potential triggers of MRR.[28] Superoxide produced by the mtETC can dismutate into the more stable H_2O_2, which may leave the mitochondria to interact with nearby sensors/organelles.[7,29–32] In agreement, MRR-inducer AA also increases superoxide production in plants, similarly to in other organisms.[33] Moreover, H_2O_2 treatment induces several MRR genes and shares overlapping transcriptomic responses with AA.[7] Central energy-metabolism-related parameters, such as ATP/adenylate and NADH/NAD^+, have also been associated with MRR initiation in different eukaryotic systems.[30] $\Delta\psi_m$ and free Ca^{2+} levels have a close physiological relationship with the mitochondrial metabolic state and hence are also potentially linked to MRR induction in plants.[34]

Here, we aimed to define which candidate physiological parameters or signaling molecules generated by mitochondria are causally responsible for triggering MRR. We assessed the dynamics of physiological parameters tightly linked to the metabolic state of mitochondria, including $MgATP^{2-}$, NADH/NAD^+ ratio, ROS/H_2O_2, Ca^{2+}, pH, $\Delta\psi_m$, and the mitochondrial oxygen consumption rate, during mitochondrial stress induced by selective chemicals/inhibitors. We selected a wide range of chemicals that inhibit mitochondrial function in various sites and therefore can alter specific parameters. By comparing the changes in physiological parameters with the induction of MRR, we eliminated most parameters as candidates for being directly involved in MRR induction. Our results indicate mitochondrial ROS (mtROS) as the most likely trigger of ANAC017-mediated MRR in plants.

RESULTS

A multi-well plate setup for monitoring cellular parameters during mitochondrial inhibition

To pinpoint the most upstream signaling components of MRR in plants, we devised an extensive experimental setup combining two main parallel approaches. First, we selected a wide range of chemicals that impinge on mitochondrial respiratory function at different sites (mtETC, ATP synthase, $\Delta\psi_m$, or TCA cycle) and identified which can induce MRR induction by RT-qPCR (Figure 1; Table S2; key resources table). We also used chemicals that induce superoxide production cell-wide (menadione) or specifically in the mitochondria (mito-paraquat [Mito-PQ]).[35,36] Second, we monitored the effects of these chemicals on energy-metabolism-related parameters using *in vivo* (real time) measurements where possible or else using isolated mitochondria (Figure 1; key resources table). Here, we employed *Arabidopsis* biosensor lines expressing specific fluorescent protein sensors to measure intracellular physiological parameters/signaling molecules[37–40] during mitochondrial inhibition in

Please cite this article in press as: Khan et al., Mitochondria-derived reactive oxygen species are the likely primary trigger of mitochondrial retrograde signaling in *Arabidopsis*, Current Biology (2023), https://doi.org/10.1016/j.cub.2023.12.005

96-well plate-based assays (key resources table; Table S1). The $MgATP^{2-}$-specific cytosolic ATeam1.03nD/nA sensor line[39] was used to measure *in vivo* cytosolic ATP levels and the roGFP2-Orp1 sensor line was used to monitor H_2O_2 dynamics,[41] while other physiological parameters were measured by specific cytosolic sensor lines: free Ca^{2+} by Cameleon NES-YC3.6,[42–44] $NADH/NAD^+$ dynamics by the NAD redox sensor Peredox-mCherry,[45] pH using cpYFP,[46] and glutathione redox potential (E_{GSH}) with Grx1-roGFP2.[47] Mitochondrial free Ca^{2+} dynamics were monitored using mitochondria-targeted YC3.6 (4mt-YC3.6).[43] Mitochondrially targeted sensor mt-roGFP2-Orp1[41] was used to monitor mitochondrial H_2O_2 dynamics, while ER-targeted Grx1-roGFP2iL-HDEL sensor was used to detect glutathione pool redox potential in the ER lumen.[48] We aimed at performing the assays in an *in vivo* context, using 5- to 7-day-old seedlings expressing the biosensors incubating in 96-well plates. For $\Delta\psi_m$ and oxygen consumption rate *in vivo*, biosensor lines are currently not available, so alternative methods were used, focusing on whole seedlings or isolated mitochondria.

To confirm MRR induction in our multi-well assays, we analyzed gene expression of alternative oxidase 1a (*AOX1a*; *At3g22370*), upregulated by oxidative stress 1 (*UPOX1*; *At2g21640*), H_2O_2 responsive gene 1 (*HRG1*, *At2g41730*), and UDP-glucosyltransferase 74E2 *(UGT74E2*; *At1g05680*), which increase during mitochondrial dysfunction in *Arabidopsis*.[7,49] Gene expression analysis was conducted in wild-type (WT) seedlings in an identical multi-well plate reader setup as the sensor line assays. This extensive setup was used to distill a detailed and time-resolved picture of MRR responses in plants (Figure 1).

Inhibition of complex III induces MRR and has widespread effects on intracellular homeostasis

AA is arguably the most extensively used chemical to induce MRR in plants.[7,50] AA binds to the quinone reduction site (Q_i) of the cytochrome bc_1 complex (complex III) and blocks electron transport from the heme b_H center to ubiquinone, leading to superoxide production at the ubiquinol oxidation site. AA is thus an appropriate positive control to test our monitoring systems. Treatment of *Arabidopsis* with 5 μM AA resulted in induction of MRR responsive genes (Figure 2A). AA treatment resulted in a significant 2- to 3-fold increase in transcript levels after 2 h for *HRG1* and for all four marker genes after 3 h. The peak expression levels were found around 4.5–6 h, as previously reported.[13,50] This demonstrated that AA efficiently induces MRR in our setup, so we evaluated the changes in physiological parameters and potential signaling molecules (Figures 1 and 2B–2E).

AA treatment resulted in a depletion in cytosolic $Mg\ ATP^{2-}$ already 10 min after treatment (Figure 2B), and a statistically significant decrease compared with mock was recorded after 20 min. ATP levels reached a low plateau after ~4 h and remained there throughout the measurements. This is consistent with mitochondria constituting the primary source of cytosolic ATP in the dark. AA also led to altered cytosolic $NADH/NAD^+$ dynamics, measured in cyt-Peredox-mCherry sensor lines (Figure 2B). A rapid increase in $NADH/NAD^+$ ratio was detected 20 min after addition of AA, indicating NADH accumulation in the cytosol due to inability of mitochondria to consume NADH after mtETC inhibition (Figure 2B). Cytosolic pH changes have also been proposed as second messengers in several plant processes.[40,51] Therefore, we investigated cytosolic pH in connection with MRR initiation in cyt-cpYFP sensor lines. A rapid acidification of the cytosol was detected in response to AA, following an almost identical pattern to cytosolic $MgATP^{2-}$. This may be due to reduced proton pumping across the plasma membrane and tonoplast (proton reserves), which is largely impaired during cytosolic ATP crisis.[51] Cytosolic free Ca^{2+} showed a slow and steady rise in response to AA that required approximately 3 h to be statistically significant These observations were comparable to previous reports, validating the setup.[34] A rapid increase in mitochondrial Ca^{2+} was also observed in response to AA (Figure 2B).

A progressive increase in H_2O_2-mediated oxidation of the cytosolic roGFP2-Orp1 sensor was observed in the presence of AA (Figure 2B). A statistically significant increase was seen after 1.5 h, and this trend continued throughout the monitoring period.

Subsequently, we examined $\Delta\psi_m$ and the mitochondrial oxygen consumption rate. *In vivo* monitoring of $\Delta\psi_m$ was performed using tetramethyl rhodamine methyl ester (TMRM) in root epidermal cells of *Arabidopsis* seedling expressing mitochondrial GFP (mito-GFP) under the confocal microscope. A high TMRM signal colocalizing with the mito-GFP fluorescence was detected in the mock treatments, suggesting a healthy $\Delta\psi_m$. However, a 1-h exposure to AA strongly dampened TMRM fluorescence (Figure 2C), indicating loss of $\Delta\psi_m$. We further confirmed rapid $\Delta\psi_m$ loss by AA in isolated mitochondria using another $\Delta\psi_m$-sensitive dye, safranin O (Figure 2D). AA also induced a considerable drop in oxygen consumption in isolated mitochondria (Figure 2E), consistent with blocking the mtETC at complex III and preventing electrons from reaching complex IV to reduce molecular O_2.

In conclusion, AA efficiently induced MRR signaling and had a significant effect on all measured parameters. Though these findings highlight the widespread effects of complex III inhibition, they unfortunately do not allow us to exclude specific parameters from being MRR triggers.

Short-term transient inhibition of the mtETC does not efficiently induce MRR

AA treatment showed rapid effects on mitochondria-related cellular parameters within 10–20 min; however, gene expression changes only became significant after 2–3 h. Many stresses induce strong gene expression responses within 10 min, including high light and touch,[52,53] so the reason for delayed transcriptional response to AA is unclear. To assess whether a short spike of inhibiting mitochondrial respiration could also trigger MRR, we treated the plants with KCN, a well-known inhibitor of complex IV. At neutral pH, KCN resides as the dissolved gas HCN, which relatively quickly leaves the liquid phase. Also, HCN diffuses more rapidly than AA into tissues. Consequently, KCN had a rapid but short-lived effect, resulting in a significant drop in $MgATP^{2-}$ already after 10 min to a level lower than that for AA. However, cytosolic ATP concentration rapidly returned to basal levels within 60 min. Similar rapid but short-lived increases in cytosolic $NADH/NAD^+$ and H_2O_2 levels were observed, as well as a $\Delta\psi_m$ decrease in isolated mitochondria

Please cite this article in press as: Khan et al., Mitochondria-derived reactive oxygen species are the likely primary trigger of mitochondrial retrograde signaling in *Arabidopsis*, Current Biology (2023), https://doi.org/10.1016/j.cub.2023.12.005

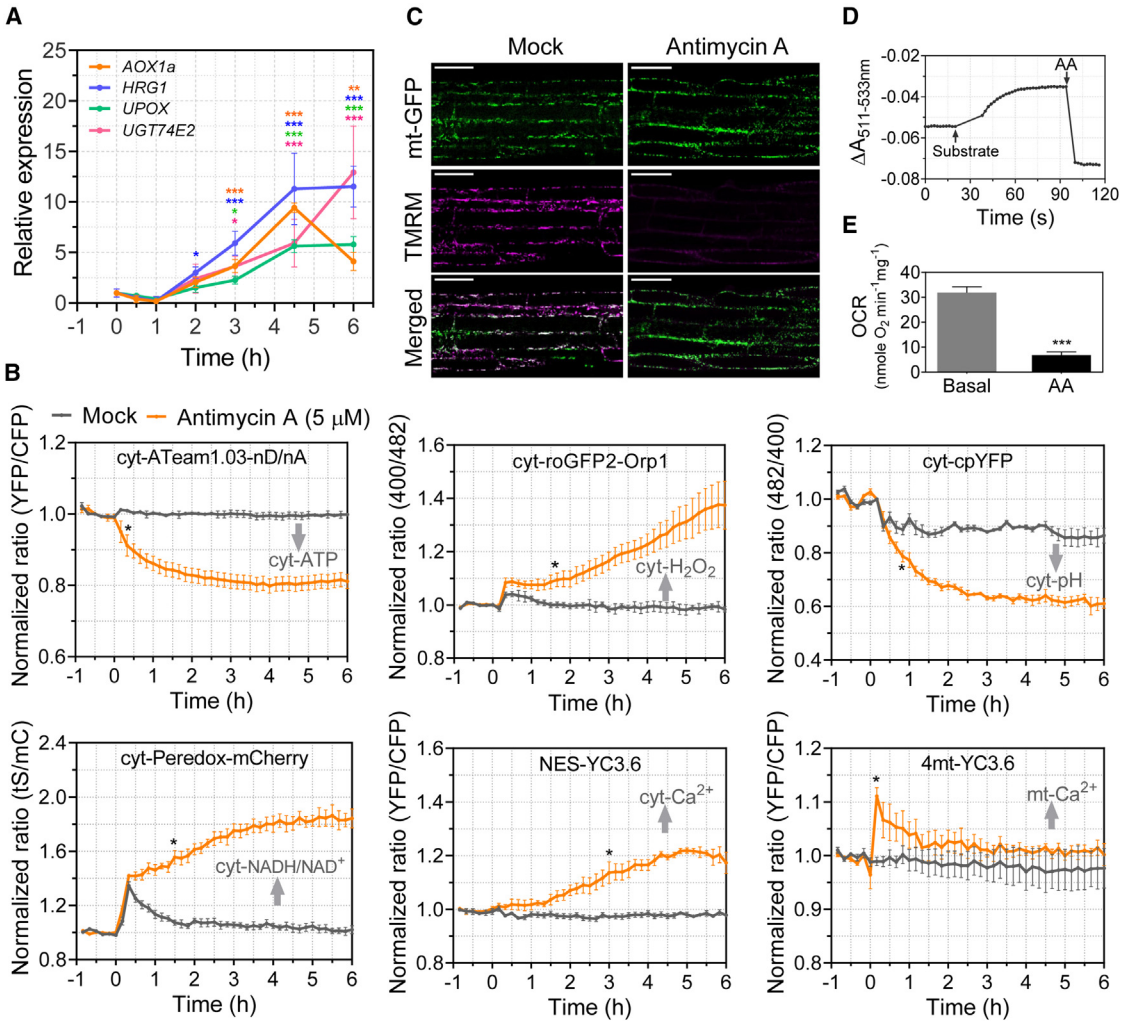

Figure 2. Antimycin A causes widespread cytosolic and mitochondrial changes and induces MRR

(A) Transcript abundance of MRR-marker genes in AA-treated seedlings (5 μM). 0 h represents samples collected just before adding chemical (after 1 h pre-incubation). Relative expression levels (ratio of treatment/mock) are shown ± SE (n = 4). Asterisks represent significant differences with mock, following gene color codes (*$p < 0.05$; **$p < 0.01$; ***$p < 0.001$).

(B) *In vivo* real-time measurement of physiological parameters in seedlings expressing fluorescent sensors. Normalized average sensor ratios after auto-fluorescence correction for indicated physiological parameters are plotted, ± SE (n = 4–6). Chemicals were added at 0 h (after 1 h pre-incubation). Up/down arrows represent significantly higher/lower levels of the parameter. Asterisks represent the first time point, with statistically significant difference in treated versus mock ($p < 0.05$).

(C) Measurement of $\Delta\psi_m$ with TMRM dye in mito-GFP root cells treated with 5 μM AA (scale bars, 50 μm).

(D) $\Delta\psi_m$ measurement in isolated mitochondria using safranin O.

(E) Oxygen consumption rate in isolated mitochondria treated with AA, ± SE (n = 3).

See also Figures S1 and S3–S7.

(Figure S1). KCN could not, however, consistently induce significant MRR gene expression changes throughout the 6 h treatment (Figure S1). Dramatic but short-lived effects on mitochondrial and cytosolic parameters by KCN were thus not sufficient to trigger substantial MRR.

We also added a second dose of KCN, 1 h after the first KCN treatment, to "prolong" or repeat the effects (Figure S1). The double application clearly resulted in two distinct peaks in cytosolic H_2O_2 formation, with H_2O_2 levels resetting within 1 h of each treatment. Neither the single nor double KCN treatment could efficiently induce MRR signaling, with only *AOX1a* showing a 2- to 3-fold induction after 2 h (peaking at 3 h) (Figure S1). Thus, inhibition of mitochondrial function apparently must be maintained for a longer time (probably 1.5–2 h) before MRR is triggered effectively.

Loss of $\Delta\psi_m$ is unlikely a direct initiator of MRR

Loss of $\Delta\psi_m$ has been suggested as the underlying trigger for MRR in yeast and animal systems.[20] Therefore, we used FCCP, an efficient ionophore and uncoupler of $\Delta\psi_m$, to test the connection between $\Delta\psi_m$ and MRR in plants in a similar setup as described for AA (Figures 2D and S1). At 5 μM, FCCP could

Please cite this article in press as: Khan et al., Mitochondria-derived reactive oxygen species are the likely primary trigger of mitochondrial retrograde signaling in *Arabidopsis*, Current Biology (2023), https://doi.org/10.1016/j.cub.2023.12.005

CellPress
OPEN ACCESS

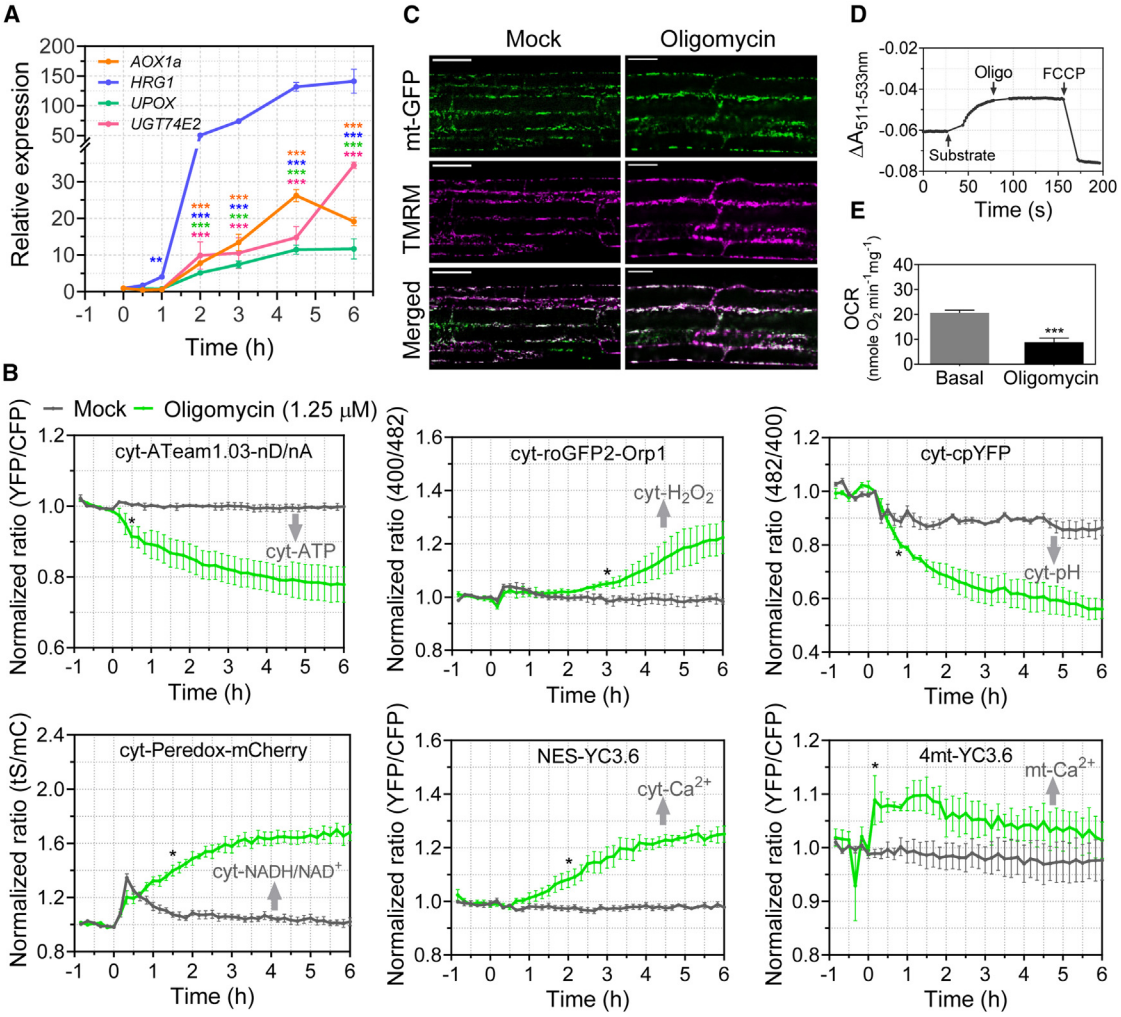

Figure 3. Inhibition of mitochondrial ATP synthase induces MRR, though $\Delta\psi_m$ is retained

(A) Expression of MRR-marker genes during oligomycin treatment, ± SE (n = 4). Asterisks represent significant differences with mock (*$p < 0.05$; **$p < 0.01$; ***$p < 0.001$).

(B) Measurement of physiological parameters in fluorescent sensor lines. Normalized average sensor ratios are plotted, ± SE value (n = 4–6). Asterisks represent the first time point, with significant difference in treated versus mock ($p < 0.05$).

(C) $\Delta\psi_m$ measurement using TMRM dye in root cells under confocal microscope (scale bars, 50 μm).

(D) $\Delta\psi_m$ measurement in isolated mitochondria using safranin O.

(E) Oxygen consumption rate in isolated mitochondria in response to oligomycin (n = 3).

See also Figures S1 and S3–S5.

partially induce MRR from 2 h after treatment (for *AOX1a* and *HRG1*) and significantly reduced ATP levels and $\Delta\psi_m$, while moderately increasing the cytosolic H_2O_2 and NADH/NAD^+ ratio. At a higher concentration of 50 μM FCCP, all tested MRR marker genes were induced after 2 h (peaking mostly after 4.5 h) and the effects on ATP, NADH/NAD^+, and cytosolic H_2O_2 levels were more pronounced (Figure S1). In conclusion, loss of $\Delta\psi_m$ by treatment with FCCP can at least partially induce MRR, but not as efficiently with the same pattern of gene inductions as, e.g., AA.

Next, we used oligomycin, which inhibits mitochondrial ATP synthase (complex V). Oligomycin binds to the F_O base plate subunit of F_OF_1 ATPase and prevents protons from passing back to the mitochondrial matrix, which is required for phosphorylation of ADP to ATP. Oligomycin strongly induced MRR at just 1.25 μM, even faster and more intensely than AA (Figure 3A). As expected, oligomycin led to a rapid decrease in cytosolic $MgATP^{2-}$ (Figure 3B). Like AA, oligomycin treatment increased cytosolic NADH/NAD^+ levels, cytosolic acidification, cytosolic/mitochondrial Ca^{2+} concentration, and cytosolic H_2O_2 (Figure 3B), while decreasing oxygen consumption (Figure 3E). Oligomycin induced a relatively slower but progressive increase in cytosolic H_2O_2 accumulation compared with AA, 3 h after treatment. However, in contrast with AA/KCN/FCCP, $\Delta\psi_m$ remained intact (even increasing slightly) in response to oligomycin treatment, as measured *in vivo* with TMRM in *Arabidopsis*

Please cite this article in press as: Khan et al., Mitochondria-derived reactive oxygen species are the likely primary trigger of mitochondrial retrograde signaling in *Arabidopsis*, Current Biology (2023), https://doi.org/10.1016/j.cub.2023.12.005

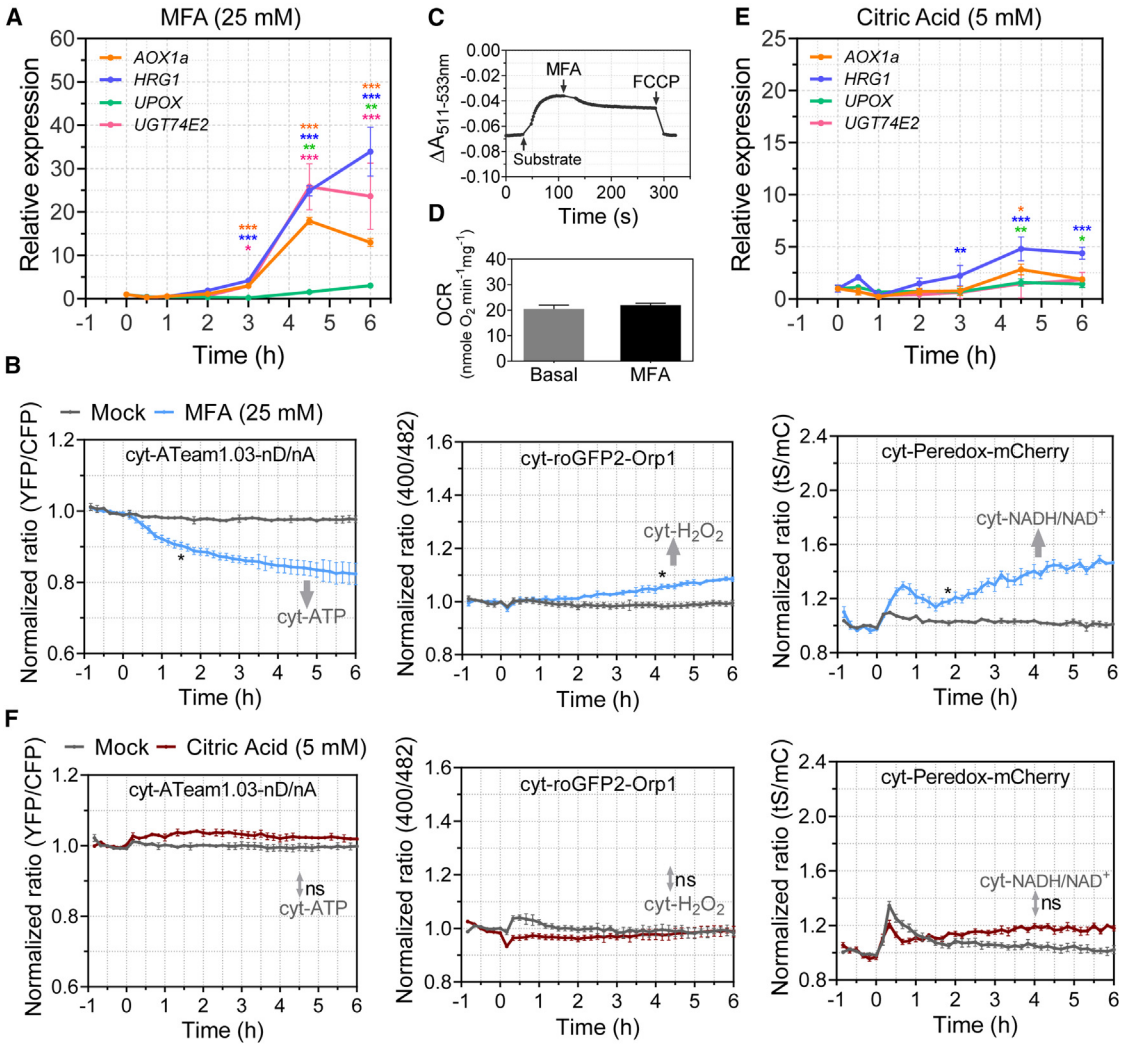

Figure 4. Monitoring of physiological and transcriptional changes in response to MFA and citrate

(A and E) Expression of MRR-marker genes during MFA and citrate treatments, respectively, ± SE (n = 4). Asterisks represent significant differences with mock, following gene color codes. (*p < 0.05; **p < 0.01; ***p < 0.001); ns, not significant.

(B and F) Measurement of physiological parameters in fluorescent sensor lines in response to MFA and citrate treatments. Normalized average sensor ratios after are plotted, ± SE value (n = 4–6). Asterisks represent the first time point, with significant difference in treated versus mock (p < 0.05), ns, not significant.

(C) $\Delta\psi_m$ measurement in response to MFA in isolated mitochondria using safranin O.

(D) Oxygen consumption rate measurements in isolated mitochondria in response to MFA (n = 3).

See also Figure S2.

seedlings and in isolated mitochondria (Figures 3C and 3D). Therefore, loss of $\Delta\psi_m$ can be ruled out as an essential MRR mediator in *Arabidopsis*.

TCA cycle intermediates are unlikely to be mediators of MRR in plants

Previous reports indicated that citrate accumulation could trigger MRR in yeast,[23] tobacco,[54,55] and *Arabidopsis*.[56] We thus investigated the impact of TCA cycle inhibition and accumulation of TCA cycle intermediates on physiological parameters and MRR. To inhibit the TCA cycle, we used monofluoroacetate (MFA). MFA inhibits *cis*-aconitase of the TCA cycle (and cytosolic aconitase), which catalyzes the conversion of citrate to isocitrate, leading to citrate accumulation.[57] In our investigation, MRR marker genes were upregulated after 3–4.5 h in response to MFA (Figure 4A), in line with previous reports.[50] Inhibiting the TCA cycle caused a comparable physiological response to ETC/complex V inhibition, such as a decrease in cytosolic ATP and increase in the NADH/NAD$^+$ ratio and cytosolic H_2O_2 levels (Figure 4B). Interestingly, similarly to the gene expression results, the majority of measured parameters took a longer time to change significantly compared with AA. The impaired carbon flow during TCA cycle inhibition may cause a more gradual effect on ETC functioning, hence delaying the MRR induction. Nevertheless, MFA could trigger a high induction of MRR genes, as previously noted.[50] Only a mild decrease in $\Delta\psi_m$ and no effect on oxygen consumption rates in isolated mitochondria were observed after treatment with MFA (Figures 4C and 4D), using

NADH as a substrate, indicating that MFA did not directly affect oxidative phosphorylation.

Because the inhibition of aconitase leads to a build-up of citrate inside the mitochondria,[57] we studied the influence of citric acid on MRR induction by exogenous application. Citrate treatment caused a substantial change in neither the expression levels of MRR-responsive genes (Figure 4E) nor the measured physiological parameters (Figure 4F).

This indicates that citrate accumulation or a reduction in the oxygen consumption rate is not the likely cause of the MRR induction and intracellular changes observed after MFA treatment. Similarly, exogenous addition of succinate (also a TCA cycle intermediate) did not cause substantial changes in MRR gene expression and measured physiological parameters (Figure S2). Previous studies also reported only very weak induction in *AOX1a* transcripts when treated with exogenous citrate and succinate in *Arabidopsis*.[56]

Excessive ROS production induces MRR marker gene expression

The above results allowed us to rule out a loss of $\Delta\psi_m$, reduced mitochondrial oxygen consumption rate, and citrate accumulation as likely direct MRR triggers. One of the common trends, however, was the accumulation of cytosolic ROS, suggesting that H_2O_2 is a potential direct MRR trigger. To assess this hypothesis, we treated the plants with menadione, a quinone-analog that causes oxidative stress across living systems, including plants.[41,58] Using the cyt-roGFP2-Orp1 biosensor line, a rapid increase in cytosolic H_2O_2 levels was already observed within 10 min of menadione treatment (Figure S2). Peak levels were reached in 20 min and gradually reached baseline after 3 h of treatment. Remarkably, menadione treatment elevated MRR-responsive genes relatively early: *UPOX* and *UGT74E2* were significantly induced already after 30 min. The peak induction of all genes was observed after 4.5 h and transcript levels returned to almost pre-treatment levels in 6 h (Figure S2). Interestingly, menadione did not change cytosolic $MgATP^{2-}$, indicating that a drop in cytosolic ATP is not required for inducing MRR in *Arabidopsis*. NADH/NAD^+ levels and cytosolic pH showed a slight decrease during menadione treatment (Figure S2). The decrease in the NADH/NAD^+ ratio was probably caused by oxidation of NAD(P)H by two-electron redox cycling of menadione.[59] A slight, slow decrease in $\Delta\psi_m$ was also seen in isolated mitochondria, but not nearly as strongly as with FCCP or AA (Figure S2). Menadione also triggered increased oxygen consumption, likely due to enhanced 1- and 2-electron autocatalytic reactions, unspecific engagement of other respiratory enzymes, and non-mitochondrial oxygen consumption.[60,61]

Mitochondria-produced ROS specifically triggers MRR in plants

As menadione generates ROS in different cellular compartments,[36] it was uncertain whether mtROS or ROS produced in other cellular compartments triggers MRR. Therefore, we used Mito-PQ to investigate the effect of mtROS in MRR induction. Mito-PQ produces ROS specifically in the mitochondria in animal systems.[35] Mito-PQ is conjugated with the lipophilic triphenyl phosphonium (TPP) cation, which selectively targets it to the mitochondrial matrix through $\Delta\psi_m$-based enrichment. There, it boosts superoxide generation toward the mitochondrial matrix through redox cycling at the flavin site of complex I in rat mitochondria.[62] We thus assessed Mito-PQ and found that it significantly induced MRR-responsive genes up to 5-fold already 2 h after treatment, while the peak levels (up to 30-fold) were reached after 4.5–6 h (Figure 5A). To control for the effects of darkness during the stress treatments, we also performed a similar experiment with 1 h pre-incubation and treatments under standard light conditions, considering the interference of AA and Mito-PQ with photosynthetic electron transport in the chloroplast. The MRR gene expression induction patterns were similar for AA under light or dark treatments (Figure S3). For Mito-PQ, a slight delay was observed in the treatment under light compared with that under dark, but the peak in expression remained around 4.5–6 h (Figure S3).

Surprisingly, Mito-PQ treatment, in contrast with the other MRR-inducing chemicals, did not impact any of the cytosolic parameters, including $MgATP^{2-}$, NADH/NAD^+, free Ca^{2+} concentration, and pH, as well as mitochondrial free Ca^{2+} concentrations (Figure 5B). This was a critical observation for defining the physiological parameters triggering MRR. Furthermore, we did not detect any change in cytosolic H_2O_2 levels, which were anticipated to increase based on the compound's description and previous studies in other systems (Figure 5B).[35,62] Mito-PQ also had no strong effect on $\Delta\psi_m$ in *Arabidopsis* seedlings, as monitored by TMRM, though a moderate drop was observed in isolated mitochondria (Figures 5C and 5D). This may be the result of transport of the conjugated TPP cation across the mitochondrial membrane, which would partially counter transmembrane potential. The oxygen consumption rate in isolated mitochondria was also unaffected by Mito-PQ, indicating that Mito-PQ has no direct negative effect on ETC activity (Figure 5E).

Based on the above, we ruled out $\Delta\psi_m$, cytosolic $MgATP^{2-}$ levels, NADH/NAD^+ dynamics, cytosolic or mitochondrial Ca^{2+} levels, and the mitochondrial oxygen consumption rate as potential MRR triggers in plants. Additionally, the menadione results had pointed to increased ROS/H_2O_2 as the only significant alteration we consistently identified as linked to induction of MRR. Intriguingly, we did not observe a change in cytosolic H_2O_2 levels in response to Mito-PQ treatment. Therefore, we hypothesized that the mtROS produced by Mito-PQ is either not reaching a sufficient level to leak into the cytosol or is detoxified by the mitochondrial/cytosolic antioxidant system. Hence, we investigated the accumulation of mitochondrial mtROS/H_2O_2 in response to the chemicals inducing MRR using the mitochondrially targeted mt-roGFP2-Orp1 sensor line[41] (Figure 6A). Oligomycin led to a rapid increase in mitochondrial H_2O_2 within 50 min of treatment, although it took 3 h to show a significant difference in cytosolic H_2O_2 levels (Figure 3B). Similar increases in mitochondrial/cytosolic H_2O_2 levels were detected with MFA (Figure 6A). FCCP resulted in a very brief decrease in H_2O_2 levels shortly after treatment, but this was reverted into elevated H_2O_2 levels after 2–3 h (Figure S1). Even though AA caused a relatively strong increase in cytosolic H_2O_2 (Figure 2B), this did not impact the redox state of the mitochondrially targeted roGFP2-Orp1 sensor protein. This is likely because AA triggers superoxide production at complex III within the inner mitochondrial membrane, and the negatively charged radical is directed toward the inside the mitochondria (IMS) due to the $\Delta\psi_m$.[63,64] Notably, mt-roGFP2-Orp1 is localized in the mitochondrial

Please cite this article in press as: Khan et al., Mitochondria-derived reactive oxygen species are the likely primary trigger of mitochondrial retrograde signaling in *Arabidopsis*, Current Biology (2023), https://doi.org/10.1016/j.cub.2023.12.005

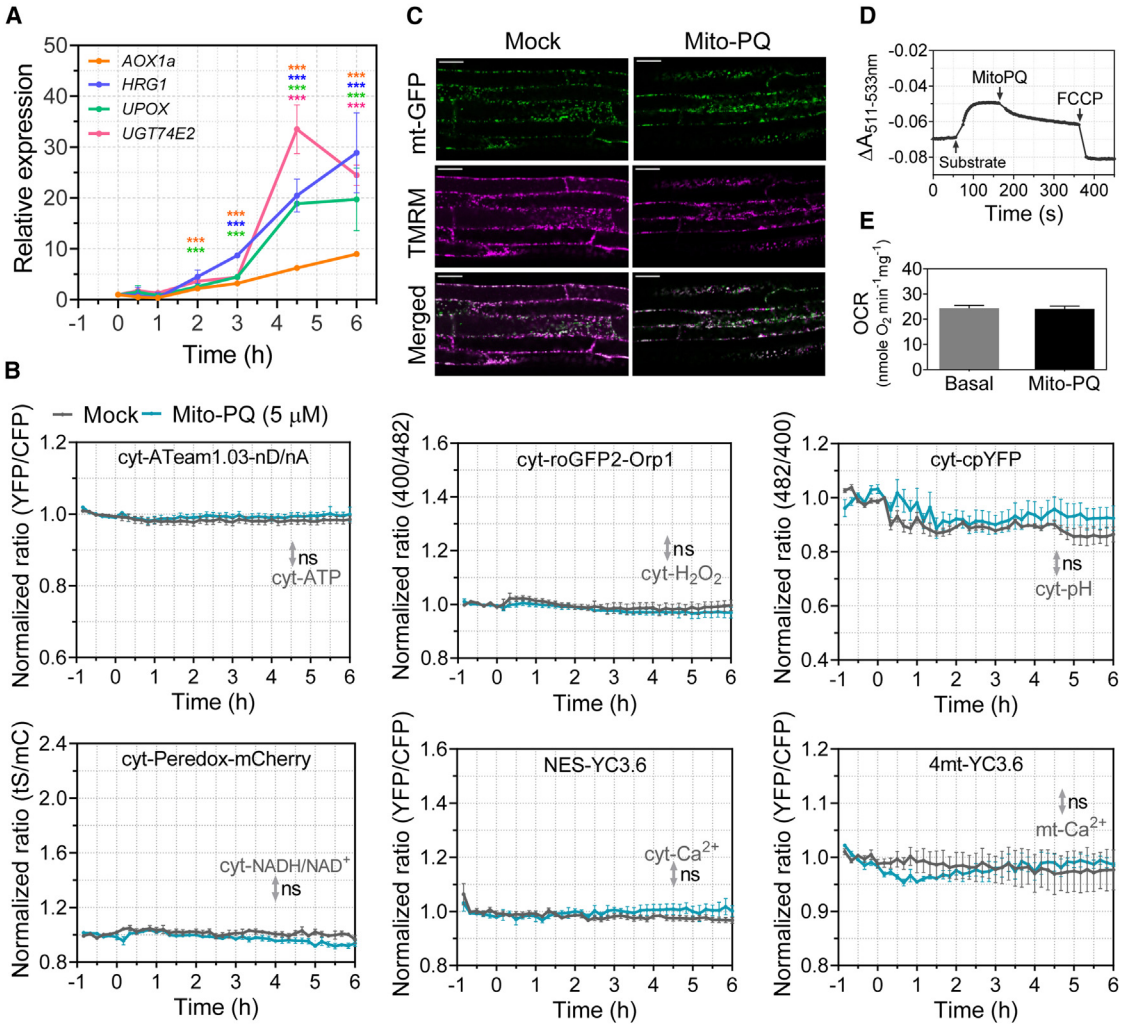

Figure 5. Mito-paraquat induces MRR signaling without affecting cytosolic parameters

(A) Expression of MRR-marker genes during Mito-PQ treatment, ± SE (n = 4). Asterisks represent significant differences with mock, following gene color codes (*p < 0.05; **p < 0.01; ***p < 0.001).

(B) Measurement of physiological parameters in fluorescent sensor lines. Normalized average sensor ratios are plotted with ± SE value (n = 4–6); ns, not significant.

(C) $\Delta\psi_m$ measurement using TMRM dye in root cells (scale bars, 50 μm).

(D) $\Delta\psi_m$ measurement in isolated mitochondria using safranin O.

(E) Oxygen consumption rate measurements in isolated mitochondria treated with Mito-PQ (n = 3).

See also Figures S2–S7.

matrix, which thus cannot efficiently detect H_2O_2 in the mitochondrial IMS. Menadione triggered a very rapid and strong increase in mtROS within 20 min (Figure 6A). Although Mito-PQ did not trigger a measurable increase in cytosolic H_2O_2 levels (Figure 5B), it did trigger a significant elevation in mtROS (Figure 6A). At 5 μM Mito-PQ, this induction came relatively late (significant after around 3 h), but the induction was more pronounced using 50 μM. Mitochondrial inhibitors thus showed different kinetics of ROS/H_2O_2 accumulation *in vivo* in the cytosol and mitochondria. This also suggests that mitochondrial inhibition primarily leads to the accumulation of ROS/H_2O_2 inside the mitochondria or IMS, which may diffuse into the cytosol. The faster accumulation of mtROS with oligomycin (Figure 6A) also correlates well with the faster induction of MRR (Figure 3A) as compared with AA (Figure 2A). The effects of AA, oligomycin, and Mito-PQ on MRR gene expression, cytosolic $MgATP^{2-}$, and H_2O_2/ROS accumulation could be reproduced in mature leaves of soil-grown plants, supporting physiological relevance (Figure S4). We also confirmed that the transfer from light to dark did not affect plate reader assay results, by repeating the most relevant sensor line experiments during the nighttime (Figure S3). The responses during the night were qualitatively similar and even showed larger amplitudes than after 1 h of transfer from light to dark, possibly because the cellular energy reserves to drive ATP production and redox systems became partially depleted in prolonged darkness.

To further confirm that these inhibitors cause an increase in mtROS/H_2O_2 production, we measured ROS/H_2O_2 in isolated

Please cite this article in press as: Khan et al., Mitochondria-derived reactive oxygen species are the likely primary trigger of mitochondrial retrograde signaling in *Arabidopsis*, Current Biology (2023), https://doi.org/10.1016/j.cub.2023.12.005

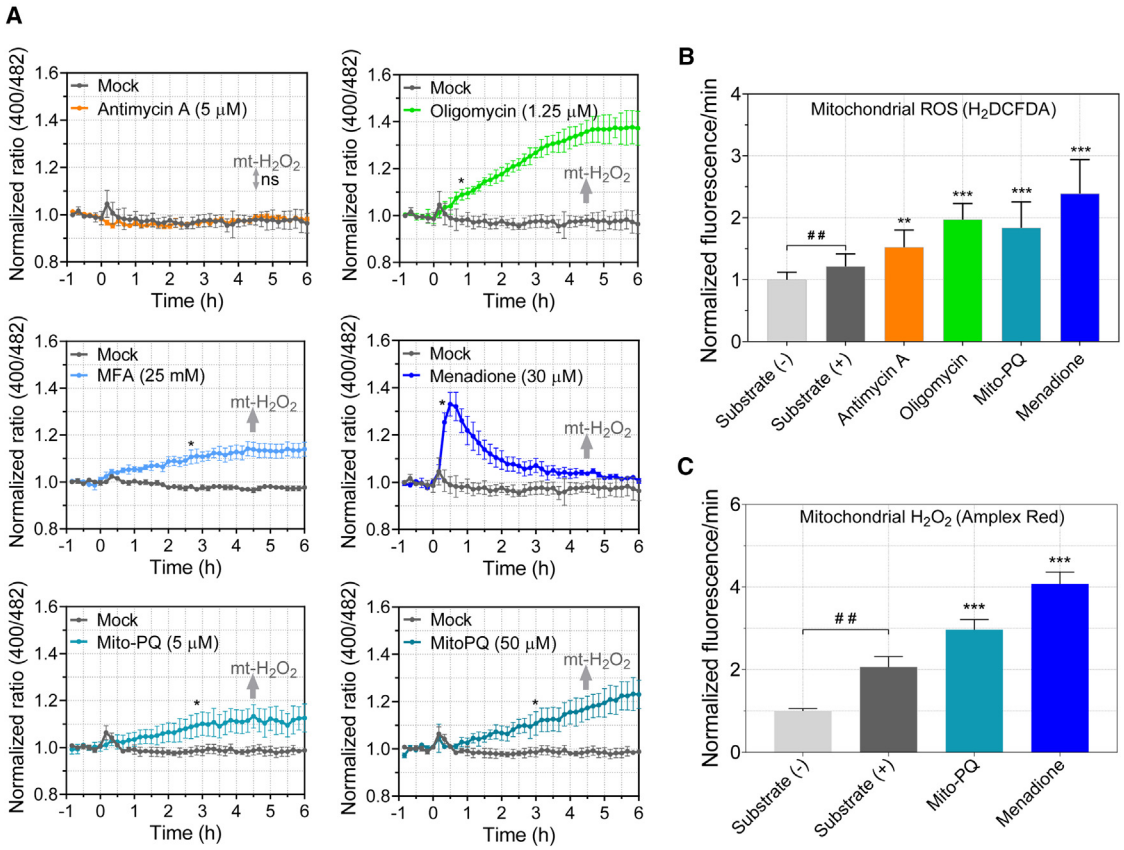

Figure 6. Mitochondrial ROS/H_2O_2 production is the likely trigger of MRR in plants

(A) Mitochondrial H_2O_2 monitoring in mt-roGFP2-Orp1 sensor line in response to indicated chemical treatments. Normalized average sensor ratios are plotted, ± SE value (n = 6–12). Asterisks represent the first time point, with significant difference in treated versus mock ($p < 0.05$).

(B and C) Mitochondrial ROS measurements in isolated mitochondria using H_2DCF-DA and Amplex Red, respectively. Data are shown as fluorescence/min with ± SE value (n = 8–12). Asterisks designate significant difference from substrate (+) control; hash symbol (#) shows significant difference between substrate (+) and (−) untreated controls. (*$p < 0.05$; **$p < 0.01$; ***$p < 0.001$); ns, not significant.

See also Figures S1–S5.

mitochondria by probing with 2′,7′-dichlorodihydrofluorescein diacetate (H_2DCF-DA). In line with the mt-roGFP2-Orp1 data, H_2DCF-DA staining showed that oligomycin, Mito-PQ, and menadione significantly increased mtROS generation (Figure 6B) compared with controls. Interestingly, DCF fluorescence measurements also showed that AA induced mtROS production by isolated mitochondria, which was not detected in mt-roGFP2-Orp1 lines, likely because H_2DCF oxidation detects ROS also inside IMS and outside of mitochondria.

We further confirmed the ability of Mito-PQ to induce mtROS using Amplex Red. Amplex Red previously detected mtROS production in isolated mitochondria with AA[33] and oligomycin.[65] Amplex Red measurements also showed significant induction in H_2O_2 levels in the presence of Mito-PQ and menadione in isolated mitochondria (Figure 6C). Together, these results confirm that mtROS production is the only parameter that showed a full correlation with MRR induction and is, thus, the most likely upstream MRR trigger.

To assess the involvement of key redox system players in MRR in plants, we measured cytosolic and mitochondrial H_2O_2 in thioredoxin (TRX) *trx-o1*, peroxiredoxin II F (*prxII F*), glutaredoxin *gr1-1* and *gr2 epc-2*, and NADPH-dependent TRX reductase (NTR) *ntra/b* mutant backgrounds expressing cyt-roGFP2-Orp1 or mt-roGFP2-Orp1.[41] Several of these lines show increased (but not saturating) sensor oxidation in the mitochondria and/or cytosol already at baseline (Figure S5) as previously observed, especially *gr1-1* and *gr2*, where glutathione redox state as a major reducing system for the biosensors is redox shifted.[47,66] Yet clear increases in H_2O_2 production were observed in the cytosol in all tested lines after AA and oligomycin treatments but not after Mito-PQ treatment. Mitochondrial sensor oxidation also increased significantly in all mutant lines after oligomycin and Mito-PQ treatments, indicating higher H_2O_2 flux. The response was smaller in *gr2*, likely because of the more oxidized redox state of mt-roGFP2-Orp1 at baseline (Figure S5). We also measured MRR gene expression in the redox mutants. These measurements were performed in lines without mitochondrial biosensors because the mt-roGFP2-Orp1 and 4mt-YC3.6 Col-0 lines showed constitutively increased expression of the MRR marker *AOX1a*, in agreement with their growth impairments[39,41] (Figure S6). Basal expression of MRR marker genes in the redox-related mutants was similar to Col-0, and in most mutants the induction of MRR genes was comparable to that in Col-0 after treatment with AA and Mito-PQ (Figure S6).

Please cite this article in press as: Khan et al., Mitochondria-derived reactive oxygen species are the likely primary trigger of mitochondrial retrograde signaling in *Arabidopsis*, Current Biology (2023), https://doi.org/10.1016/j.cub.2023.12.005

In *gr1-1* and *ntra/b*, an impaired induction of gene expression was observed for some MRR marker genes. The increased oxidation state of roGFP2-Orp1 in these mutants may intuitively lead to the expectation of increased MRR gene expression. Because this is not the case, we speculate that the impact on the redox systems in those mutants (Figure S5) likely affects many redox interactors, making it impossible to pinpoint any specific mechanism at this stage. In *prxII F* mutants, there was a slight decrease in MRR marker gene induction after AA and Mito-PQ treatment. Given the role of mitochondrial PRXII F in peroxide detoxification and the ability of peroxiredoxins to act as H_2O_2 sensors, we repeated the gene expression assay in an extended time course. However, *prxII F* MRR induction levels were largely comparable to those in Col-0 (Figure S7), indicating that mitochondrial PRXII F does not have a major role in sensing matrix H_2O_2 signals in the mode of MRR studied here.

As Mito-PQ was indicated to receive electrons from complex I to produce superoxide in animal mitochondria,[62] impairing complex I might potentially lower superoxide production by Mito-PQ. We isolated mitochondria of the *ndufs4* complex I mutant[67] and measured ROS production in response to Mito-PQ using Amplex Red. Surprisingly, Mito-PQ resulted in much higher H_2O_2 production in the *ndufs4* background than in WT (Figure S5). As in yeast mitochondria (which lack complex I), paraquat receives electrons from alternative type-II dehydrogenases,[68] which are upregulated in *ndufs4* mutants[67]; these may contribute to the higher Mito-PQ-induced ROS production. Inhibition of complex I with rotenone also increased superoxide production by paraquat in mammalian systems.[68] Elevated superoxide was previously also suggested, based on nitroblue tetrazolium (NBT) tissue staining in *ndufs4* mutants.[67] In agreement, we observed higher basal expression of MRR genes in *ndufs4* plants (Figure S6), as previously reported.[69] These findings underline that mitochondrially produced H_2O_2 is the likely trigger of MRR in plants.

Redox changes in the ER lumen are not required for ANAC017-mediated MRR signaling

The transcription factor ANAC017 plays a crucial role in MRR signaling in plants.[4,7,13] Though Mito-PQ can induce MRR marker expression, this does not necessarily mean that the induction is mediated via ANAC017. Therefore, we treated WT, *anac017-KO (anac017-1)*, and *anac017-EMS* (*rao2.1*) mutants with Mito-PQ and measured MRR marker expression. Consistently, the transcript levels of all four MRR marker genes were strongly induced in Col-0 seedlings 4.5 h after spraying Mito-PQ. Remarkably, this Mito-PQ-triggered induction was strongly repressed in both *anac017* mutants compared with Col-0 (Figure 7A). A slight induction of MRR was still observed after 4.5 h in *anac017* mutants, which is likely due to partial redundancy with, e.g., ANAC013.[13,14,50] H_2O_2 production in isolated mitochondria of *anac017* mutants was similar to WT before and after treatment with Mito-PQ or menadione (Figure S5), indicating that the lower MRR induction is not due to a lack of mtROS production. Therefore, Mito-PQ induces MRR via the ANAC017-dependent pathway.

ANAC017 was shown to be anchored into the ER membrane via a C-terminal transmembrane domain and the N-terminal domain relocates to the nucleus after cleavage by rhomboid proteases.[7,14,70] The actual trigger that mediates ANAC017 cleavage is, however, unknown. It is thus tempting to speculate that mitochondrially produced H_2O_2 needs to reach the ER to transmit the mitochondrial signal, for instance, via ER-mitochondria contact sites.[71,72] To measure this, we used the recently published ER-targeted Grx1-roGFP2iL-HDEL line in which the roGFP2 moiety was modified to function within the oxidizing ER lumen conditions.[48] We also used the cytosolic Grx1-roGFP2 sensor line to monitor cytosolic glutathione redox potential (E_{GSH}). Consistent with our cytosolic roGFP2-Orp1 sensor data, AA and oligomycin treatment led to an oxidation of the cytosolic glutathione pool, while no change was observed in presence of Mito-PQ (Figure 7B). Although AA and oligomycin caused oxidation of the ER lumen, Grx1-roGFP2iL-HDEL could not detect an altered redox state in the ER lumen after treatment with Mito-PQ (Figure 7C). Taken together, our study shows that superoxide or H_2O_2 produced inside mitochondria are the most likely primary mediator of MRR in plants. The results also indicate that no substantial leakage of mtROS into the cytosol or ER lumen appears to be needed to initiate the signaling cascade, unlike what was previously suggested.[12,30]

DISCUSSION

Because many cellular parameters are closely inter-linked with the functional state of mitochondria, one treatment can influence several parameters,[30] making them hard to disentangle. We found that mtETC and TCA cycle inhibition influence a similar set of parameters, including ATP status, $\Delta\psi_m$, NADH/NAD^+ ratio, and ROS/H_2O_2 levels. Also, an uncoupler like FCCP impacts on these parameters. Mito-PQ could, however, only clearly affect mtROS formation, while typical mitochondrial performance indicators, including $MgATP^{2-}$, free Ca^{2+} levels, pH, and cytosolic/ER lumen ROS, remained unchanged. Nevertheless, Mito-PQ induced gene expression changes via the ANAC017-dependent MRR pathway. This provides compelling evidence that mtROS is a primary trigger to initiate ANAC017-dependent MRR in plants, while other parameters affected may often be correlated but not directly involved. AA induces changes in thousands of genes within 3 h,[7] but these changes may be the result of many signaling pathways being triggered by changes in, e.g., ATP status, of which ANAC017-mediated MRR is one. Recent literature highlights the role of mtROS in mediating MRR in several model systems. In yeast, ATP was identified as main trigger for RTG2-based RTG signaling[16]; however, current evidence suggests ROS modulates the RTG2-dependent RTG pathway.[73–75] In addition to the "drop in membrane potential/release of mitochondrial Ca^{2+}" model in metazoans, recent studies have experimentally established a significant role of mtROS in MRR in *Drosophila*,[76] *C. elegans* (via eIF2 alpha kinase GCN-2, hypoxia inducible factor-1 [HIF-1α], and respiratory enzyme CLK-1),[77–79] cultured human cells, hepatoma Hep3B cells (via HIF-1),[80] colorectal carcinoma cells (via NF-κB),[81] and neurons and glial cells.[82] Moreover, exogenous H_2O_2 can activate MRR-specific transcripts in an overlapping transcriptional response with AA in *Arabidopsis*.[7,83] As initially proposed based on similarities between the transcriptomic responses to mitochondrial inhibitors and hypoxia,[83] several studies have now indicated the

Please cite this article in press as: Khan et al., Mitochondria-derived reactive oxygen species are the likely primary trigger of mitochondrial retrograde signaling in *Arabidopsis*, Current Biology (2023), https://doi.org/10.1016/j.cub.2023.12.005

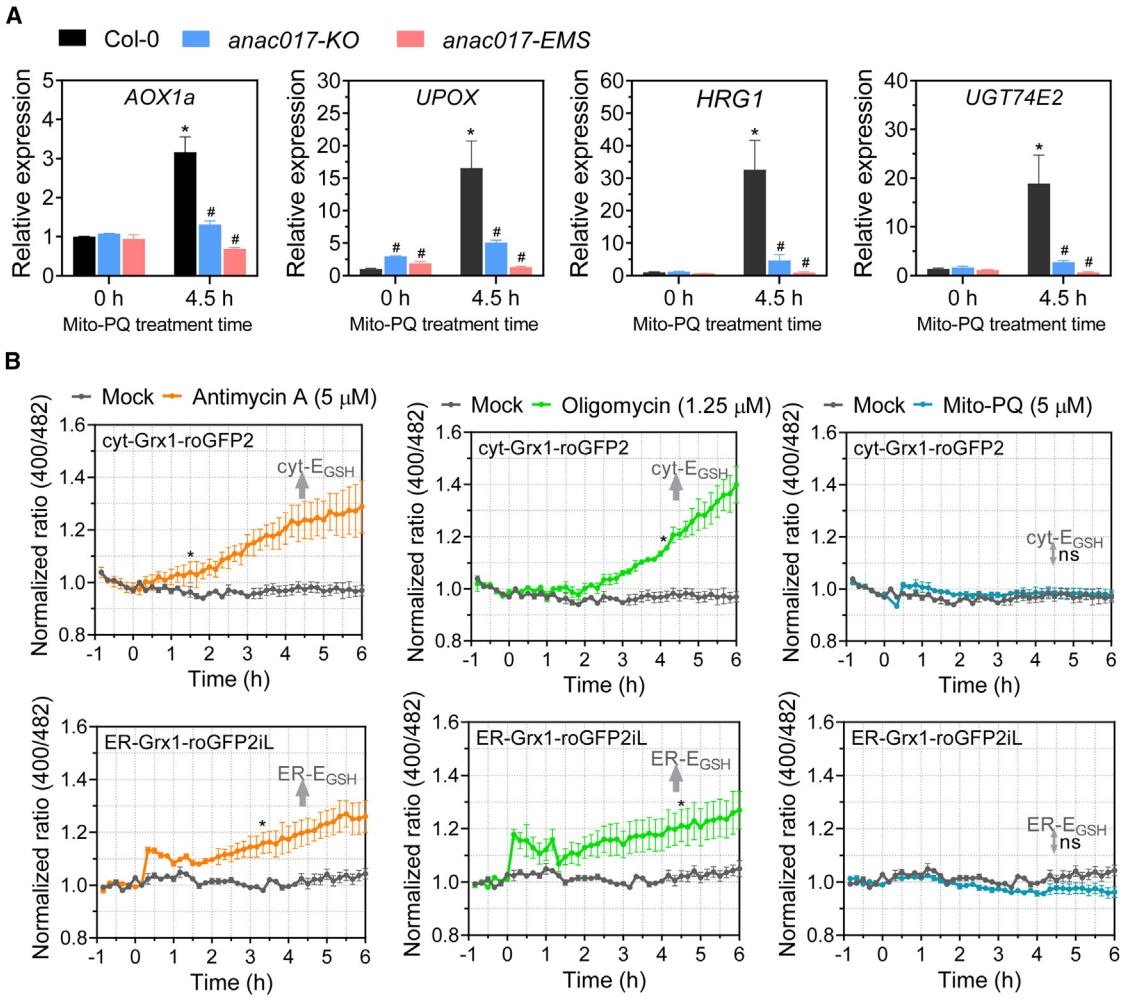

Figure 7. Mito-PQ-induced mitochondrial ROS trigger MRR induction via the ANAC017-pathway

(A) Expression of MRR-marker genes in Col-0, *anac017-KO*, and *anac017-EMS* before and after 4.5 h of Mito-PQ treatment, ± SE value (n = 4). Asterisks denote significant difference in Col-0 treated versus 0 h, hash symbol (#) represents significant difference between Col-0 and mutants at the same time point (*/#$p < 0.001$).

(B) Monitoring of glutathione redox potential in the cytosol and ER lumen in response to indicated chemicals. Normalized average sensor ratios were plotted, ± SE value (n = 4–6). Asterisks represent the first time point with significant difference in treated versus mock ($p < 0.05$).

See also Figures S5–S7.

physiological importance of ANAC013/17-mediated MRR during submergence and hypoxia in plants.[14,84,85]

Currently, it remains unclear how mtROS activates retrograde signaling in these different systems, although the significance of mtROS in plant growth, development, and stress responses has been highlighted.[86,87] The superoxide generated by mtETC has a very short lifetime and cannot permeate the mitochondrial membrane, making it suitable for rapid detection by potential intra-organellar superoxide sensors. Proteins containing iron-sulfur (Fe-S) clusters are common in electron transfer reactions and function as co-factors in several enzymes; hence, they could act as primary superoxide sensors.[30,88,89] For instance, ROS can reversibly inactivate Fe-S containing aconitase in animal and plant systems, allowing the enzyme to act as redox sensor by controlling the metabolic flux inside mitochondria.[30,57,88,90,91] Furthermore, our results also showed that inhibition of aconitase by MFA leads to MRR induction in *Arabidopsis*.[92]

H_2O_2, the more stable and more abundant ROS, could directly interact with specific thiol-reactive redox proteins, including transcription factors, which regulate the expression of H_2O_2-sensitive/stress responsive genes.[30,93–95] Cys-peroxidases in the mitochondrial matrix, such as PRXII F and glutathione peroxidase-like 6 (GPXL6) in *Arabidopsis*, may act in both peroxide detoxification and sensing.[96] Both peroxidases can act as sinks for electrons from the TRX/NTR system, making them potential sensors that relay H_2O_2 signals to the TRX system. Recent studies have identified the mitochondrial TRX system as a regulator of redox-switches on oxidative phosphorylation components and of TCA cycle flux.[97–102] Although the Cys-based redoxin system appears to play an important role in regulating the mitochondrial redox and energy machineries, our results do not support the conclusion that PRXII F or the Cys-based redoxin system are themselves central components of MRR and mitochondrial H_2O_2 signaling.

It was also proposed that oxidation of mitochondrial proteins during oxidative stress can trigger proteolysis and that the broken oxidized peptides may transduce organellar signals.[103,104] Therefore, further research should focus on identifying targets of these systems in the context of MRR.

Apart from intra-mitochondrial sensors, experimental evidence in animal systems suggests that mitochondrial H_2O_2 can be directly perceived by sensors located in the IMS to trigger phosphorylation cascades or can be sensed by sensors located close to the mitochondrial surface.[105] In this scenario, mitochondrial-ER contact sites look well suited for ANAC017-dependent MRR induction.[106,107] However, we could not detect changes in the redox state of the cytosol or ER lumen after Mito-PQ treatment, suggesting that substantial change in ER-lumen redox state by direct transfer of mtROS is not required to activate ER-localized ANAC017. Furthermore, the relatively short ROS burst induced with KCN was also insufficient to induce MRR, suggesting that it takes at least 1–2 h of "stress" before the ANAC017-pathway changes gene expression. This suggests that some buffering capacity or threshold level must be overcome before the signaling is fully activated. ROS produced inside mitochondria may be rapidly buffered by mitochondria-localized antioxidant systems to adjust mitochondrial functions. However, more prolonged oxidative stress could trigger excessive oxidation of thiol-based redox "sensor" proteins, post-translational modifications, leakage of degraded peptides from oxidized proteins, inhibition of mitochondrial proteins, etc. This could transduce the signal to other compartments such as the ER to activate ANAC017. A recent study in mammalian systems indicated very steep gradients of H_2O_2 coming from mitochondria that may not reach far in the cell.[32] Possibly, MRR-inducing mtROS may be sensed very closely to the outer mitochondrial surface, without altering bulk cytosolic H_2O_2 levels.

H_2O_2 and singlet oxygen are also mediators of chloroplast retrograde signaling. During high light stress, it was suggested that chloroplasts in close proximity to the nucleus may pass on H_2O_2 directly into the nucleus to activate gene expression.[108] Singlet oxygen produced in chloroplasts can also change retrograde gene expression, by oxidizing a Trp^{643} residue on Executer1, which makes it prone to proteolytic degradation by chloroplast membrane-bound FtsH proteins.[109,110] Further research is thus needed to pinpoint the downstream signaling steps of ROS to activate MRR in plants.

In summary, our work indicates that ROS produced inside mitochondria is the most likely primary trigger to initiate MRR in plants. Additionally, this work provides detailed insights into mitochondria-related physiological parameters under various mitochondrial perturbations, which will be useful for future mitochondrial research.

STAR★METHODS

Detailed methods are provided in the online version of this paper and include the following:

SUPPLEMENTAL INFORMATION

Supplemental information can be found online at https://doi.org/10.1016/j.cub.2023.12.005.

ACKNOWLEDGMENTS

We thank Dr. Ola Gustafsson for technical assistance with confocal microscopy analysis. We thank Andreas J. Meyer for providing the Grx1-roGFP2iL-HDEL sensor line. We thank Prof. Ian Max Møller for his critical comments on the project. This project was supported by the Swedish Research Council (Vetenskapsrådet 2017-03854, 2021-04358), Crafoord Foundation (20170862), Carl Trygger Foundation (CTS 17: 487; CTS 22: 1981), Carl Tesdorpf Stiftelse, and NovoNordiskFonden (NNF18OC0034822). K.K. was supported by the Sven and Lilly Lawski fund (N2022-0019), Wenner-Gren foundation (UPD2019-0211), and Royal Physiographic Society of Lund. This work was supported by Piano di Sviluppo di Ateneo 2019 (University of Milan) (to A.C.) and by a PhD fellowship from the University of Milan (to S.B.).

AUTHOR CONTRIBUTIONS

O.V.A., K.K., A.G.R., M.S., and A.C. conceived and planned the project. K.K., H.C.T., B.M., P.Ö., and S.B. performed experiments. K.K. and O.V.A. analyzed data. K.K. and O.V.A. wrote the manuscript with input from all co-authors.

DECLARATION OF INTERESTS

The authors declare no competing interests.

Received: April 19, 2023
Revised: October 28, 2023
Accepted: December 4, 2023
Published: January 3, 2024

REFERENCES

1. Welchen, E., García, L., Mansilla, N., and Gonzalez, D.H. (2014). Coordination of plant mitochondrial biogenesis: keeping pace with cellular requirements. Front. Plant Sci. *4*, 551.
2. Wang, Y., Berkowitz, O., Selinski, J., Xu, Y., Hartmann, A., and Whelan, J. (2018). Stress responsive mitochondrial proteins in *Arabidopsis* thaliana. Free Radic. Biol. Med. *122*, 28–39.
3. Van Aken, O., and Whelan, J. (2012). Comparison of transcriptional changes to chloroplast and mitochondrial perturbations reveals common and specific responses in *Arabidopsis*. Front. Plant Sci. *3*, 281.
4. De Clercq, I., Vermeirssen, V., Van Aken, O., Vandepoele, K., Murcha, M.W., Law, S.R., Inzé, A., Ng, S., Ivanova, A., Rombaut, D., et al. (2013). The membrane-bound NAC transcription factor ANAC013 functions in mitochondrial retrograde regulation of the oxidative stress response in *Arabidopsis*. Plant Cell *25*, 3472–3490.
5. Zhang, B., Van Aken, O., Thatcher, L., De Clercq, I., Duncan, O., Law, S.R., Murcha, M.W., Van der Merwe, M., Seifi, H.S., and Carrie, C. (2014). The mitochondrial outer membrane AAA ATPase at OM 66 affects

cell death and pathogen resistance in Arabidopsis thaliana. Plant J. *80*, 709–727.

6. Tognetti, V.B., Van Aken, O., Morreel, K., Vandenbroucke, K., van de Cotte, B., De Clercq, I., Chiwocha, S., Fenske, R., Prinsen, E., Boerjan, W., et al. (2010). Perturbation of indole-3-butyric acid homeostasis by the UDP-glucosyltransferase UGT74E2 modulates *Arabidopsis* architecture and water stress tolerance. Plant Cell *22*, 2660–2679.
7. Ng, S., Ivanova, A., Duncan, O., Law, S.R., Van Aken, O., De Clercq, I., Wang, Y., Carrie, C., Xu, L., Kmiec, B., et al. (2013). A membrane-bound NAC transcription factor, ANAC017, mediates mitochondrial retrograde signaling in *Arabidopsis*. Plant Cell *25*, 3450–3471.
8. Gong, F., Yao, Z., Liu, Y., Sun, M., and Peng, X. (2021). H_2O_2 response gene 1/2 are novel sensors or responders of H2O2 and involve in maintaining embryonic root meristem activity in *Arabidopsis* thaliana. Plant Sci. *310*, 11098.
9. Skirycz, A., De Bodt, S., Obata, T., De Clercq, I., Claeys, H., De Rycke, R., Andriankaja, M., Van Aken, O., Van Breusegem, F., Fernie, A.R., and Inze, D. (2010). Developmental stage specificity and the role of mitochondrial metabolism in the response of *Arabidopsis* leaves to prolonged mild osmotic stress. Plant Physiol. *152*, 226–244.
10. Dahal, K., and Vanlerberghe, G.C. (2017). Alternative oxidase respiration maintains both mitochondrial and chloroplast function during drought. New Phytol. *213*, 560–571.
11. Vanlerberghe, G.C. (2013). Alternative oxidase: a mitochondrial respiratory pathway to maintain metabolic and signaling homeostasis during abiotic and biotic stress in plants. Int. J. Mol. Sci. *14*, 6805–6847.
12. Ng, S., De Clercq, I., Van Aken, O., Law, S.R., Ivanova, A., Willems, P., Giraud, E., Van Breusegem, F., and Whelan, J. (2014). Anterograde and retrograde regulation of nuclear genes encoding mitochondrial proteins during growth, development, and stress. Mol. Plant *7*, 1075–1093.
13. Broda, M., Khan, K., O'Leary, B., Pružinská, A., Lee, C.P., Millar, A.H., and Van Aken, O. (2021). Increased expression of ANAC017 primes for accelerated senescence. Plant Physiol. *186*, 2205–2221.
14. Eysholdt-Derzsó, E., Renziehausen, T., Frings, S., Frohn, S., von Bongartz, K., Igisch, C.P., Mann, J., Häger, L., Macholl, J., and Leisse, D. (2023). Endoplasmic reticulum–bound ANAC013 factor is cleaved by RHOMBOID-LIKE 2 during the initial response to hypoxia in *Arabidopsis* thaliana. Proc. Natl. Acad. Sci. USA. *120*, e2221308120.
15. Tran, H.C., and Van Aken, O. (2020). Mitochondrial unfolded protein-related responses across kingdoms: similar problems, different regulators. Mitochondrion *53*, 166–177.
16. Zhang, F., Pracheil, T., Thornton, J., and Liu, Z.C. (2013). Adenosine triphosphate (ATP) is a candidate signaling molecule in the mitochondria-to-nucleus retrograde response pathway. Genes-Basel *4*, 86–100.
17. Ždralević, M., Guaragnella, N., and Giannattasio, S. (2015). Yeast as a tool to study mitochondrial retrograde pathway en route to cell stress response. Methods Mol. Biol. *1265*, 321–331.
18. da Cunha, F.M., Torelli, N.Q., and Kowaltowski, A.J. (2015). Mitochondrial retrograde signaling: triggers, pathways, and outcomes. Oxid. Med. Cell. Longev. *2015*, 482582.
19. Sekito, T., Liu, Z.C., Thornton, J., and Butow, R.A. (2002). RTG-dependent mitochondria-to-nucleus signaling is regulated by MKS1 and is linked to formation of yeast prion [URE3]. Mol. Biol. Cell *13*, 795–804.
20. Miceli, M.V., Jiang, J.C., Tiwari, A., Rodriguez-Quiñones, J.F., and Jazwinski, S.M. (2011). Loss of mitochondrial membrane potential triggers the retrograde response extending yeast replicative lifespan. Front. Genet. *2*, 102.
21. Biswas, G., Adebanjo, O.A., Freedman, B.D., Anandatheerthavarada, H.K., Vijayasarathy, C., Zaidi, M., Kotlikoff, M., and Avadhani, N.G. (1999). Retrograde Ca2+ signaling in C2C12 skeletal myocytes in response to mitochondrial genetic and metabolic stress: a novel mode of inter-organelle crosstalk. EMBO J. *18*, 522–533.
22. Biswas, G., Anandatheerthavarada, H.K., and Avadhani, N.G. (2003). Mechanism of mitochondrial stress induced resistance to apoptosis in mtDNA depleted C2C12 cells. FASEB J. *17*, A680–A681.
23. Butow, R.A., and Avadhani, N.G. (2004). Mitochondrial signaling: the retrograde response. Mol. Cell *14*, 1–15.
24. Melber, A., and Haynes, C.M. (2018). UPR(mt) regulation and output: a stress response mediated by mitochondrial-nuclear communication. Cell Res. *28*, 281–295.
25. Chakrabarti, A., Chen, A.W., and Varner, J.D. (2011). A review of the mammalian unfolded protein response. Biotechnol. Bioeng. *108*, 2777–2793.
26. Houtkooper, R.H., Mouchiroud, L., Ryu, D., Moullan, N., Katsyuba, E., Knott, G., Williams, R.W., and Auwerx, J. (2013). Mitonuclear protein imbalance as a conserved longevity mechanism. Nature *497*, 451–457.
27. Itoh, K., Wakabayashi, N., Katoh, Y., Ishii, T., Igarashi, K., Engel, J.D., and Yamamoto, M. (1999). Keap1 represses nuclear activation of antioxidant responsive elements by Nrf2 through binding to the amino-terminal Neh2 domain. Genes Dev. *13*, 76–86.
28. Kohli, S.K., Khanna, K., Bhardwaj, R., Abd Allah, E.F., Ahmad, P., and Corpas, F.J. (2019). Assessment of subcellular ROS and NO metabolism in higher plants: multifunctional signaling molecules. Antioxidants (Basel) *8*, 641.
29. Maxwell, D.P., Wang, Y., and McIntosh, L. (1999). The alternative oxidase lowers mitochondrial reactive oxygen production in plant cells. Proc. Natl. Acad. Sci. USA *96*, 8271–8276.
30. Schwarzländer, M., and Finkemeier, I. (2013). Mitochondrial energy and redox signaling in plants. Antioxid. Redox Signal. *18*, 2122–2144.
31. Schwarzländer, M., König, A.C., Sweetlove, L.J., and Finkemeier, I. (2012). The impact of impaired mitochondrial function on retrograde signaling: a meta-analysis of transcriptomic responses. J. Exp. Bot. *63*, 1735–1750.
32. Hoehne, M.N., Jacobs, L.J.H.C., Lapacz, K.J., Calabrese, G., Murschall, L.M., Marker, T., Kaul, H., Trifunovic, A., Morgan, B., and Fricker, M. (2022). Spatial and temporal control of mitochondrial H2O2 release in intact human cells. EMBO J. *41*, e109169.
33. Belt, K., Huang, S., Thatcher, L.F., Casarotto, H., Singh, K.B., Van Aken, O., and Millar, A.H. (2017). Salicylic acid-dependent plant stress signaling via mitochondrial succinate dehydrogenase. Plant Physiol. *173*, 2029–2040.
34. Wagner, S., De Bortoli, S., Schwarzländer, M., and Szabò, I. (2016). Regulation of mitochondrial calcium in plants versus animals. J. Exp. Bot. *67*, 3809–3829.
35. Chowdhury, A.R., Zielonka, J., Kalyanaraman, B., Hartley, R.C., Murphy, M.P., and Avadhani, N.G. (2020). Mitochondria-targeted paraquat and metformin mediate ROS production to induce multiple pathways of retrograde signaling: a dose-dependent phenomenon. Redox Biol. *36*, 101606.
36. Loor, G., Kondapalli, J., Schriewer, J.M., Chandel, N.S., Vanden Hoek, T.L.V., and Schumacker, P.T. (2010). Menadione triggers cell death through ROS-dependent mechanisms involving PARP activation without requiring apoptosis. Free Radic. Biol. Med. *49*, 1925–1936.
37. Walia, A., Waadt, R., and Jones, A.M. (2018). Genetically encoded biosensors in plants: pathways to discovery. Annu. Rev. Plant Biol. *69*, 497–524.
38. Schwarzländer, M., Dick, T.P., Meyer, A.J., and Morgan, B. (2016). Dissecting redox biology using fluorescent protein sensors. Antioxid. Redox Signal. *24*, 680–712.
39. De Col, V., Fuchs, P., Nietzel, T., Elsässer, M., Voon, C.P., Candeo, A., Seeliger, I., Fricker, M.D., Grefen, C., Møller, I.M., et al. (2017). ATP sensing in living plant cells reveals tissue gradients and stress dynamics of energy physiology. eLife *6*, e26770.
40. Wagner, S., Steinbeck, J., Fuchs, P., Lichtenauer, S., Elsässer, M., Schippers, J.H.M., Nietzel, T., Ruberti, C., Van Aken, O., Meyer, A.J., et al. (2019). Multiparametric real-time sensing of cytosolic physiology

links hypoxia responses to mitochondrial electron transport. New Phytol. *224*, 1668–1684.

41. Nietzel, T., Elsässer, M., Ruberti, C., Steinbeck, J., Ugalde, J.M., Fuchs, P., Wagner, S., Ostermann, L., Moseler, A., Lemke, P., et al. (2019). The fluorescent protein sensor roGFP2-Orp1 monitors in vivo H_2O_2 and thiol redox integration and elucidates intracellular H_2O_2 dynamics during elicitor-induced oxidative burst in *Arabidopsis*. New Phytol. *221*, 1649–1664.
42. Krebs, M., Held, K., Binder, A., Hashimoto, K., Den Herder, G., Parniske, M., Kudla, J., and Schumacher, K. (2012). FRET-based genetically encoded sensors allow high-resolution live cell imaging of Ca^{2+} dynamics. Plant J. *69*, 181–192.
43. Loro, G., Drago, I., Pozzan, T., Lo Schiavo, F.L., Zottini, M., and Costa, A. (2012). Targeting of Cameleons to various subcellular compartments reveals a strict cytoplasmic/mitochondrial Ca2+ handling relationship in plant cells. Plant J. *71*, 1–13.
44. Loro, G., Wagner, S., Doccula, F.G., Behera, S., Weinl, S., Kudla, J., Schwarzländer, M., Costa, A., and Zottini, M. (2016). Chloroplast-specific in vivo Ca^{2+} imaging using yellow cameleon fluorescent protein sensors reveals organelle-autonomous Ca^{2+} signatures in the stroma. Plant Physiol. *171*, 2317–2330.
45. Steinbeck, J., Fuchs, P., Negroni, Y.L., Elsässer, M., Lichtenauer, S., Stockdreher, Y., Feitosa-Araujo, E., Kroll, J.B., Niemeier, J.-O., and Humberg, C. (2020). In vivo NADH/NAD+ biosensing reveals the dynamics of cytosolic redox metabolism in plants. Plant Cell *32*, 3324–3345.
46. Schwarzländer, M., Wagner, S., Ermakova, Y.G., Belousov, V.V., Radi, R., Beckman, J.S., Buettner, G.R., Demaurex, N., Duchen, M.R., and Forman, H.J. (2014). The 'mitoflash'probe cpYFP does not respond to superoxide. Nature *514*, E12–E14.
47. Marty, L., Siala, W., Schwarzländer, M., Fricker, M.D., Wirtz, M., Sweetlove, L.J., Meyer, Y., Meyer, A.J., Reichheld, J.P., and Hell, R. (2009). The NADPH-dependent thioredoxin system constitutes a functional backup for cytosolic glutathione reductase in *Arabidopsis*. Proc. Natl. Acad. Sci. USA *106*, 9109–9114.
48. Ugalde, J.M., Aller, I., Kudrjasova, L., Schmidt, R.R., Schlößer, M., Homagk, M., Fuchs, P., Lichtenauer, S., Schwarzländer, M., Müller-Schüssele, S.J., et al. (2022). Endoplasmic reticulum oxidoreductin provides resilience against reductive stress and hypoxic conditions by mediating luminal redox dynamics. Plant Cell *34*, 4007–4027.
49. Van Aken, O., Ford, E., Lister, R., Huang, S., and Millar, A.H. (2016). Retrograde signaling caused by heritable mitochondrial dysfunction is partially mediated by ANAC017 and improves plant performance. Plant J. *88*, 542–558.
50. Van Aken, O., De Clercq, I., Ivanova, A., Law, S.R., Van Breusegem, F., Millar, A.H., and Whelan, J. (2016). Mitochondrial and chloroplast stress responses are modulated in distinct touch and chemical inhibition phases. Plant Physiol. *171*, 2150–2165.
51. Felle, H.H. (2001). pH: signal and messenger in plant cells. Plant Biol. *3*, 577–591.
52. Van Moerkercke, A., Duncan, O., Zander, M., Šimura, J., Broda, M., Vanden Bossche, R., Lewsey, M.G., Lama, S., Singh, K.B., Ljung, K., et al. (2019). A MYC2/MYC3/MYC4-dependent transcription factor network regulates water spray-responsive gene expression and jasmonate levels. Proc. Natl. Acad. Sci. USA *116*, 23345–23356.
53. Vogel, M.O., Moore, M., König, K., Pecher, P., Alsharafa, K., Lee, J., and Dietz, K.-J. (2014). Fast retrograde signaling in response to high light involves metabolite export, mitogen-activated PROTEIN KINASE6, and AP2/ERF transcription factors in *Arabidopsis*. Plant Cell *26*, 1151–1165.
54. Vanlerberghe, G.C., Day, D.A., Wiskich, J.T., Vanlerberghe, A.E., and McIntosh, L. (1995). Alternative oxidase activity in tobacco leaf mitochondria (dependence on tricarboxylic acid cycle-mediated redox regulation and pyruvate activation). Plant Physiol. *109*, 353–361.
55. Gray, G.R., Maxwell, D.P., Villarimo, A.R., and McIntosh, L. (2004). Mitochondria/nuclear signaling of alternative oxidase gene expression occurs through distinct pathways involving organic acids and reactive oxygen species. Plant Cell Rep. *23*, 497–503.
56. Finkemeier, I., König, A.-C., Heard, W., Nunes-Nesi, A., Pham, P.A., Leister, D., Fernie, A.R., and Sweetlove, L.J. (2013). Transcriptomic analysis of the role of carboxylic acids in metabolite signaling in *Arabidopsis* leaves. Plant Physiol. *162*, 239–253.
57. Gupta, K.J., Shah, J.K., Brotman, Y., Jahnke, K., Willmitzer, L., Kaiser, W.M., Bauwe, H., and Igamberdiev, A.U. (2012). Inhibition of aconitase by nitric oxide leads to induction of the alternative oxidase and to a shift of metabolism towards biosynthesis of amino acids. J. Exp. Bot. *63*, 1773–1784.
58. Li, J., Zuo, X., Cheng, P., Ren, X.Y., Sun, S.B., Xu, J.Q., Holmgren, A., and Lu, J. (2019). The production of reactive oxygen species enhanced with the reduction of menadione by active thioredoxin reductase. Metallomics *11*, 1490–1497.
59. Jarabak, R., and Jarabak, J. (1995). Effect of ascorbate on the DT-diaphorase-mediated redox cycling of 2-methyl-1, 4-naphthoquinone. Arch. Biochem. Biophys. *318*, 418–423.
60. Kakimoto, P.A., Serna, J.D.C., de Miranda Ramos, V., Zorzano, A., and Kowaltowski, A.J. (2021). Increased glycolysis is an early consequence of palmitate lipotoxicity mediated by redox signaling. Redox Biol. *45*, 102026.
61. Acworth, I.N. (2003). The Handbook of Redox Biochemistry.
62. Robb, E.L., Gawel, J.M., Aksentijević, D., Cochemé, H.M., Stewart, T.S., Shchepinova, M.M., Qiang, H., Prime, T.A., Bright, T.P., James, A.M., et al. (2015). Selective superoxide generation within mitochondria by the targeted redox cycler MitoParaquat. Free Radic. Biol. Med. *89*, 883–894.
63. Bleier, L., and Dröse, S. (2013). Superoxide generation by complex III: from mechanistic rationales to functional consequences. Biochim. Biophys. Acta-Bioenerg. *1827*, 1320–1331.
64. Brand, M.D. (2016). Mitochondrial generation of superoxide and hydrogen peroxide as the source of mitochondrial redox signaling. Free Radic. Biol. Med. *100*, 14–31.
65. Jardim-Messeder, D., Margis-Pinheiro, M., and Sachetto-Martins, G. (2022). Salicylic acid and adenine nucleotides regulate the electron transport system and ROS production in plant mitochondria. Biochim. Biophys. Acta Bioenerg. *1863*, 148559.
66. Marty, L., Bausewein, D., Müller, C., Bangash, S.A.K., Moseler, A., Schwarzländer, M., Müller-Schüssele, S.J., Zechmann, B., Riondet, C., and Balk, J. (2019). *Arabidopsis* glutathione reductase 2 is indispensable in plastids, while mitochondrial glutathione is safeguarded by additional reduction and transport systems. New Phytol. *224*, 1569–1584.
67. Meyer, E.H., Tomaz, T., Carroll, A.J., Estavillo, G., Delannoy, E., Tanz, S.K., Small, I.D., Pogson, B.J., and Millar, A.H. (2009). Remodeled respiration in ndufs4 with low phosphorylation efficiency suppresses *Arabidopsis* germination and growth and alters control of metabolism at night. Plant Physiol. *151*, 603–619.
68. Cochemé, H.M., and Murphy, M.P. (2008). Complex I is the major site of mitochondrial superoxide production by paraquat. J. Biol. Chem. *283*, 1786–1798.
69. Padavannil, A., Ayala-Hernandez, M.G., Castellanos-Silva, E.A., and Letts, J.A. (2021). The mysterious multitude: structural perspective on the accessory subunits of respiratory complex I. Front. Mol. Biosci. *8*, 798353.
70. Wang, M., Wang, M., Zhao, M., Wang, M., Liu, S., Tian, Y., Moon, B., Liang, C., Li, C., and Shi, W. (2022). TaSRO1 plays a dual role in suppressing TaSIP1 to fine tune mitochondrial retrograde signaling and enhance salinity stress tolerance. New Phytol. *236*, 495–511.
71. Liu, L., and Li, J. (2019). Communications between the endoplasmic reticulum and other organelles during abiotic stress response in plants. Front. Plant Sci. *10*, 749.

72. Michaud, M., and Jouhet, J. (2019). Lipid trafficking at membrane contact sites during plant development and stress response. Front. Plant Sci. *10*, 2.

73. Guaragnella, N., Ždralević, M., Lattanzio, P., Marzulli, D., Pracheil, T., Liu, Z., Passarella, S., Marra, E., and Giannattasio, S. (2013). Yeast growth in raffinose results in resistance to acetic-acid induced programmed cell death mostly due to the activation of the mitochondrial retrograde pathway. Biochim. Biophys. Acta *1833*, 2765–2774.

74. Pan, Y., Schroeder, E.A., Ocampo, A., Barrientos, A., and Shadel, G.S. (2011). Regulation of yeast chronological life span by TORC1 via adaptive mitochondrial ROS signaling. Cell Metab. *13*, 668–678.

75. Torelli, N.Q., Ferreira-Júnior, J.R., Kowaltowski, A.J., and da Cunha, F.M. (2015). RTG1-and RTG2-dependent retrograde signaling controls mitochondrial activity and stress resistance in Saccharomyces cerevisiae. Free Radic. Biol. Med. *81*, 30–37.

76. Owusu-Ansah, E., Yavari, A., Mandal, S., and Banerjee, U. (2008). Distinct mitochondrial retrograde signals control the G1-S cell cycle checkpoint. Nat. Genet. *40*, 356–361.

77. Baker, B.M., Nargund, A.M., Sun, T., and Haynes, C.M. (2012). Protective coupling of mitochondrial function and protein synthesis via the eIF2α kinase GCN-2. PLOS Genet. *8*, e1002760.

78. Lee, S.J., Hwang, A.B., and Kenyon, C. (2010). Inhibition of respiration extends C. elegans life span via reactive oxygen species that increase HIF-1 activity. Curr. Biol. *20*, 2131–2136.

79. Monaghan, R.M., Barnes, R.G., Fisher, K., Andreou, T., Rooney, N., Poulin, G.B., and Whitmarsh, A.J. (2015). A nuclear role for the respiratory enzyme CLK-1 in regulating mitochondrial stress responses and longevity. Nat. Cell Biol. *17*, 782–792.

80. Chandel, N.S., Maltepe, E., Goldwasser, E., Mathieu, C.E., Simon, M.C., and Schumacker, P.T. (1998). Mitochondrial reactive oxygen species trigger hypoxia-induced transcription. Proc. Natl. Acad. Sci. USA *95*, 11715–11720.

81. Formentini, L., Sánchez-Aragó, M., Sánchez-Cenizo, L., and Cuezva, J.M. (2012). The mitochondrial ATPase inhibitory factor 1 triggers a ROS-mediated retrograde prosurvival and proliferative response. Mol. Cell *45*, 731–742.

82. Granat, L., Hunt, R.J., and Bateman, J.M. (2020). Mitochondrial retrograde signaling in neurological disease. Philos. Trans. R. Soc. Lond. B Biol. Sci. *375*, 20190415.

83. Wagner, S., Van Aken, O., Elsässer, M., and Schwarzländer, M. (2018). Mitochondrial energy signaling and its role in the low-oxygen stress response of plants. Plant Physiol. *176*, 1156–1170.

84. Bui, L.T., Shukla, V., Giorgi, F.M., Trivellini, A., Perata, P., Licausi, F., and Giuntoli, B. (2020). Differential submergence tolerance between juvenile and adult *Arabidopsis* plants involves the ANAC017 transcription factor. Plant J. *104*, 979–994.

85. Meng, X., Li, L., Narsai, R., De Clercq, I., Whelan, J., and Berkowitz, O. (2020). Mitochondrial signaling is critical for acclimation and adaptation to flooding in *Arabidopsis* thaliana. Plant J. *103*, 227–247.

86. Huang, S., Van Aken, O., Schwarzländer, M., Belt, K., and Millar, A.H. (2016). The roles of mitochondrial reactive oxygen species in cellular signaling and stress response in plants. Plant Physiol. *171*, 1551–1559.

87. Van Aken, O. (2021). Mitochondrial redox systems as central hubs in plant metabolism and signaling. Plant Physiol. *186*, 36–52.

88. Read, A.D., Bentley, R.E.T., Archer, S.L., and Dunham-Snary, K.J. (2021). Mitochondrial iron-sulfur clusters: structure, function, and an emerging role in vascular biology. Redox Biol. *47*, 102164.

89. Przybyla-Toscano, J., Christ, L., Keech, O., and Rouhier, N. (2021). Iron sulfur proteins in plant mitochondria: roles and maturation. J. Exp. Bot. *72*, 2014–2044.

90. Verniquet, F., Gaillard, J., Neuburger, M., and Douce, R. (1991). Rapid inactivation of plant aconitase by hydrogen peroxide. Biochem. J. *276*, 643–648.

91. Hartl, M., and Finkemeier, I. (2012). Plant mitochondrial retrograde signaling: post-translational modifications enter the stage. Front. Plant Sci. *3*, 253.

92. Umbach, A.L., Zarkovic, J., Yu, J., Ruckle, M.E., McIntosh, L., Hock, J.J., Bingham, S., White, S.J., George, R.M., Subbaiah, C.C., and Rhoads, D.M. (2012). Comparison of intact *Arabidopsis thaliana* leaf transcript profiles during treatment with inhibitors of mitochondrial electron transport and TCA cycle. PLoS One *7*, e44339.

93. Cui, F., Brosché, M., Shapiguzov, A., He, X.Q., Vainonen, J.P., Leppälä, J., Trotta, A., Kangasjärvi, S., Salojärvi, J., Kangasjärvi, J., et al. (2019). Interaction of methyl viologen-induced chloroplast and mitochondrial signaling in *Arabidopsis*. Free Radic. Biol. Med. *134*, 555–566.

94. Liu, J., Li, Z., Wang, Y., and Xing, D. (2014). Overexpression of ALTERNATIVE OXIDASE1a alleviates mitochondria-dependent programmed cell death induced by aluminium phytotoxicity in *Arabidopsis*. J. Exp. Bot. *65*, 4465–4478.

95. Dourmap, C., Roque, S., Morin, A., Caubrière, D., Kerdiles, M., Béguin, K., Perdoux, R., Reynoud, N., Bourdet, L., Audebert, P.A., et al. (2020). Stress signaling dynamics of the mitochondrial electron transport chain and oxidative phosphorylation system in higher plants. Ann. Bot. *125*, 721–736.

96. Klupczyńska, E.A., Dietz, K.J., Małecka, A., and Ratajczak, E. (2022). Mitochondrial peroxiredoxin-IIF (PRXIIF) activity and function during seed aging. Antioxidants (Basel) *11*, 1226.

97. Yoshida, K., Noguchi, K., Motohashi, K., and Hisabori, T. (2013). Systematic exploration of thioredoxin target proteins in plant mitochondria. Plant Cell Physiol. *54*, 875–892.

98. Schmidtmann, E., König, A.-C., Orwat, A., Leister, D., Hartl, M., and Finkemeier, I. (2014). Redox regulation of *Arabidopsis* mitochondrial citrate synthase. Mol. Plant *7*, 156–169.

99. Yoshida, K., and Hisabori, T. (2014). Mitochondrial isocitrate dehydrogenase is inactivated upon oxidation and reactivated by thioredoxin-dependent reduction in *Arabidopsis*. Front. Environ. Sci. *2*, 38.

100. Daloso, D.M., Müller, K., Obata, T., Florian, A., Tohge, T., Bottcher, A., Riondet, C., Bariat, L., Carrari, F., and Nunes-Nesi, A. (2015). Thioredoxin, a master regulator of the tricarboxylic acid cycle in plant mitochondria. Proc. Natl. Acad. Sci. USA *112*, E1392–E1400.

101. Florez-Sarasa, I., Obata, T., Del-Saz, N.S.F.N., Reichheld, J.-P., Meyer, E.H., Rodriguez-Concepcion, M., Ribas-Carbo, M., and Fernie, A.R. (2019). The lack of mitochondrial thioredoxin TRXo1 affects in vivo alternative oxidase activity and carbon metabolism under different light conditions. Plant Cell Physiol. *60*, 2369–2381.

102. Nietzel, T., Mostertz, J., Ruberti, C., Née, G., Fuchs, P., Wagner, S., Moseler, A., Müller-Schüssele, S.J., Benamar, A., and Poschet, G. (2020). Redox-mediated kick-start of mitochondrial energy metabolism drives resource-efficient seed germination. Proc. Natl. Acad. Sci. USA *117*, 741–751.

103. Møller, I.M., and Sweetlove, L.J. (2010). ROS signaling–specificity is required. Trends Plant Sci. *15*, 370–374.

104. Tan, Y.-F., O'Toole, N., Taylor, N.L., and Millar, A.H. (2010). Divalent metal ions in plant mitochondria and their role in interactions with proteins and oxidative stress-induced damage to respiratory function. Plant Physiol. *152*, 747–761.

105. Patterson, H.C., Gerbeth, C., Thiru, P., Vögtle, N.F., Knoll, M., Shahsafaei, A., Samocha, K.E., Huang, C.X., Harden, M.M., and Song, R. (2015). A respiratory chain controlled signal transduction cascade in the mitochondrial intermembrane space mediates hydrogen peroxide signaling. Proc. Natl. Acad. Sci. USA *112*, E5679–E5688.

106. Mueller, S.J., and Reski, R. (2015). Mitochondrial dynamics and the ER: the plant perspective. Front. Cell Dev. Biol. *3*, 78.

107. Jaipargas, E.-A., Barton, K.A., Mathur, N., and Mathur, J. (2015). Mitochondrial pleomorphy in plant cells is driven by contiguous ER dynamics. Front. Plant Sci. *6*, 783.

108. Exposito-Rodriguez, M., Laissue, P.P., Yvon-Durocher, G., Smirnoff, N., and Mullineaux, P.M. (2017). Photosynthesis-dependent H2O2 transfer from chloroplasts to nuclei provides a high-light signaling mechanism. Nat. Commun. *8*, 49.

109. Dogra, V., Duan, J., Lee, K.P., Lv, S., Liu, R., and Kim, C. (2017). FtsH2-dependent proteolysis of EXECUTER1 is essential in mediating singlet oxygen-triggered retrograde signaling in *Arabidopsis thaliana*. Front. Plant Sci. *8*, 1145.

110. Dogra, V., Li, M., Singh, S., Li, M., and Kim, C. (2019). Oxidative post-translational modification of EXECUTER1 is required for singlet oxygen sensing in plastids. Nat. Commun. *10*, 2834.

111. Logan, D.C., and Leaver, C.J. (2000). Mitochondria-targeted GFP highlights the heterogeneity of mitochondrial shape, size and movement within living plant cells. J. Exp. Bot. *51*, 865–871.

112. Reichheld, J.-P., Khafif, M., Riondet, C., Droux, M., Bonnard, G., and Meyer, Y. (2007). Inactivation of thioredoxin reductases reveals a complex interplay between thioredoxin and glutathione pathways in *Arabidopsis* development. Plant Cell *19*, 1851–1865.

113. Finkemeier, I., Goodman, M., Lamkemeyer, P., Kandlbinder, A., Sweetlove, L.J., and Dietz, K.-J. (2005). The mitochondrial type II peroxiredoxin F is essential for redox homeostasis and root growth of *Arabidopsis thaliana* under stress. J. Biol. Chem. *280*, 12168–12180.

114. Queval, G., Issakidis-Bourguet, E., Hoeberichts, F.A., Vandorpe, M., Gakière, B., Vanacker, H., Miginiac-Maslow, M., Van Breusegem, F., and Noctor, G. (2007). Conditional oxidative stress responses in the *Arabidopsis* photorespiratory mutant cat2 demonstrate that redox state is a key modulator of daylength-dependent gene expression, and define photoperiod as a crucial factor in the regulation of H2O2-induced cell death. Plant J. *52*, 640–657.

115. Schindelin, J., Arganda-Carreras, I., Frise, E., Kaynig, V., Longair, M., Pietzsch, T., Preibisch, S., Rueden, C., Saalfeld, S., Schmid, B., et al. (2012). Fiji: an open-source platform for biological-image analysis. Nat. Methods *9*, 676–682.

116. Broda, M., and Van Aken, O. (2018). Studying retrograde signaling in plants. In Plant Programmed Cell Death (Springer), pp. 73–85.

117. Tran, H.C., and Van Aken, O. (2022). Purification of leaf mitochondria from *Arabidopsis thaliana* using Percoll density gradients. Methods Mol. Biol. *2363*, 1–12.

118. Lyu, W., Selinski, J., Li, L., Day, D.A., Murcha, M.W., Whelan, J., and Wang, Y. (2018). Isolation and respiratory measurements of mitochondria from *Arabidopsis thaliana*. J. Vis. Exp. *131*.

119. Moore, A.L., and Bonner, W.D. (1982). Measurements of membrane-potentials in plant-mitochondria with the safranine method. Plant Physiol. *70*, 1271–1276.

120. Smith, A.M., Ratcliffe, R.G., and Sweetlove, L.J. (2004). Activation and function of mitochondrial uncoupling protein in plants. J. Biol. Chem. *279*, 51944–51952.

Please cite this article in press as: Khan et al., Mitochondria-derived reactive oxygen species are the likely primary trigger of mitochondrial retrograde signaling in *Arabidopsis*, Current Biology (2023), https://doi.org/10.1016/j.cub.2023.12.005

STAR★METHODS

KEY RESOURCES TABLE

REAGENT or RESOURCE	SOURCE	IDENTIFIER
Chemicals, peptides, and recombinant proteins		
Antimycin A from *Streptomyces sp*.	Sigma-Aldrich	Cat. No.: A8674
Oligomycin from *Streptomyces diastatochromogenes*	Sigma-Aldrich	Cat. No.: O4876
Potassium Cyanide	Sigma-Aldrich	Cat. No.: 1.04965
FCCP (Carbonyl cyanide 4-(trifluoromethoxy) phenylhydrazone)	Sigma-Aldrich	Cat. No.: C2920
Menadione	Sigma-Aldrich	Cat. No.: M9429
Citric Acid	Sigma-Aldrich	Cat. No.: 1002440500
Safranin O	Sigma-Aldrich	Cat. No.: S2255
Succinic acid	Thermo Scientific	Cat. No.: 158742500
Mito PQ (MitoParaquat)	MedChemExpress	Cat. No.: HY-130278
Monofluoroacetate (MFA)	MP Biomedicals	Cat. No.: ICN201080
TMRM	Thermo Scientific	Cat. No.: T668
H_2DCF-DA	Thermo Scientific	Cat. No.: D399
Critical commercial assays		
Spectrum Plant Total RNA Kit	Sigma-Aldrich	Cat. No.: STRN250
iScript cDNA Synhesis Kit	Bio-Rad	Cat. No.: 1708891
SsoAdvanced Universal SYBR Green Supermix	Bio-Rad	Cat. No.: 1725274
CFX 384 Real Time System	Bio-Rad	NA
Amplex Red Hydrogen Peroxide/Peroxidase Assay Kit	Thermo Scientific	Cat. No.: A22188
Experimental models: Cell lines		
Arabidopsis thaliana, Ecotype: Columbia (Col-0)	Widely distributed	N/A
Experimental models: Organisms/strains		
Arabidopsis thaliana (Col-0)	Widely distributed	N/A
Arabidopsis: cyt-ATeam1.03-nD/nA	De Col et al.[39]	N/A
Arabidopsis: cyt/mt-roGFP2-Orp1	Nietzel et al.[41]	N/A
Arabidopsis: cyt-Grx1-roGFP2	Marty et al.[47]	N/A
Arabidopsis: Grx1-roGFP2iL-HDEL	Ugalde et al.[48]	N/A
Arabidopsis: Peredox-mCherry	Steinbeck et al.[45]	N/A
Arabidopsis: cyt-NES-YC3.6	Krebs et al.[42]; Loro et al.[43]	N/A
Arabidopsis: 4mt-YC3.6	Loro et al.[43]	N/A
Arabidopsis: cyt-cpYFP	Schwarzländer et al.[46]	N/A
Arabidopsis: mito-GFP	Logan and Leaver[111]	N/A
Arabidopsis: *gr1*	Marty et al.[47]	SALK_105794
Arabidopsis: *gr2 epc-2*	Marty et al.[66]	N/A
Arabidopsis: *trx-o1*	Daloso et al.[100]	SALK 042792
Arabidopsis: *ntra/b*	Reichheld et al.[112]	N/A
Arabidopsis: *prxII F*	Finkemeier et al.[113]	GK-114G01
Arabidopsis: *cat2*	Queval et al.[114]	SALK_057998.55.00
Arabidopsis: *ndufs4*	Meyer et al.[67]	SAIL_596_E11
Arabidopsis: *anac017*-KO/TDNA (anac017-1)	Ng et al.[7]	SALK_022174
Arabidopsis: *anac017*-EMS (rao2.1)	Ng et al.[7]	N/A
Arabidopsis:*gr1* cyt/mt-roGFP2-Orp1	Nietzel et al.[41]	N/A
Arabidopsis: *gr2 epc-2* cyt/mt-roGFP2-Orp1	Nietzel et al.[41]	N/A
Arabidopsis: *trx-o1* cyt/mt-roGFP2-Orp1	Nietzel et al.[41]	N/A
Arabidopsis: *ntra/b* cyt/mt-roGFP2-Orp1	Nietzel et al.[41]	N/A

(*Continued on next page*)

Please cite this article in press as: Khan et al., Mitochondria-derived reactive oxygen species are the likely primary trigger of mitochondrial retrograde signaling in *Arabidopsis*, Current Biology (2023), https://doi.org/10.1016/j.cub.2023.12.005

Continued

REAGENT or RESOURCE	SOURCE	IDENTIFIER
Arabidopsis: *prxII F* cyt/mt-roGFP2-Orp1	Nietzel et al.[41]	N/A
Arabidopsis: *cat2* cyt/mt-roGFP2-Orp1	Nietzel et al.[41]	N/A
Oligonucleotides:		
See Table S3	N/A	N/A
Software and algorithms		
Prism	GraphPad Software, USA	www.graphpad.com
ImageJ	Schindelin et al.[115]	https://imagej.nih.gov/ij/index.html

RESOURCE AVAILABILITY

Lead contact

Additional details and requests for resources and reagents should be directed toward the lead contact, Olivier Van Aken (olivier.van_aken@biol.lu.se).

Materials availability

The plant materials used in this study are available upon request.

Data and code availability

- All data reported in this paper will be shared by the lead contact upon request.
- This study does not report original code.
- Any additional information required to reanalyze the data reported in this paper is available from the lead contact upon request.

EXPERIMENTAL MODEL AND SUBJECT DETAILS

Arabidopsis seeds were dry sterilized by chlorine gas and sown on square plates containing half-strength Murashige and Skoog medium (MS) supplemented with 1 % (w/v) sucrose, 0.5 g/L MES, and 0.8% (w/v) plant agar (pH 5.8). The seeds were stratified for 2 days at 4 °C in dark before being transferred to the growth room under long day conditions (22°C, 16-hour light/8-hour dark cycle, 100 μmol m^{-2} s^{-1}). Mature *Arabidopsis* plants were grown by sowing seeds in pots filled with a soil mixture consisting of soil, perlite, and vermiculite in a 4:1:1 ratio, followed by a 2-day cold stratification at 4°C. Subsequently, the plants were grown under long day conditions. Information on all plant lines used in this study is listed in the key resources table.

METHOD DETAILS

Multiwell plate reader setup

For the plate reader assays, 7-day-old seedlings were transferred into 96-well black Nunc plates (Thermo Fisher Scientific, 137101) (5 seedlings per well) containing 200 μL assay medium (10 mM MES, 10 mM $MgCl_2$, 10 mM $CaCl_2$, 5 mM KCl, pH 5.8). Fluorescence data were acquired using a CLARIOstar Plus plate reader (BMG Labtech, Ortenberg, Germany) pre-equilibrated to 25°C. Measurements were performed according to Wagner et al.[40] with orbital averaging mode for 40-50 excitation light flashes on a circle of 4-5 mm radius without shaking. The seedlings were excited with monochromatic light at specific wavelengths and emissions were recorded according to the fluorescent sensor proteins shown in the Table S1 and key resources table. To avoid the effects of photosynthesis and short-term dark transfer, seedlings were pre-incubated for 1 h in the dark inside the plate reader. Before treatments, a baseline was established using pre-run fluorescence data. The measurements were then paused, chemicals (key resources table) were added and mixed under safe (green) light, and the plate was reinserted into the plate reader to resume measurements. The working concentrations of different chemicals are indicated in Table S2. At each time point, background corrections were performed by subtracting the autofluorescence of WT seedlings (present on the same plate) from the obtained sensor fluorescence data. The data were further normalized to their respective "pre-run" data for graphical presentation of the results. For measurements in mature leaves, leaf discs of 4-week-old soil-grown plants were placed in the 96-well plate wells for 1 h pre-incubation in the dark, similarly to the standard assays on young seedlings (Figure S6). Statistically significant differences between mock and treated were determined by two-way ANOVA with Bonferroni's multiple comparisons test.

For expression analysis of MRR-responsive genes, 7-day-old *Arabidopsis thaliana* WT (Col-0) seedlings were treated in identical experimental conditions as in the fluorometric monitoring, and samples were collected at various time points after chemical and mock treatments (Table S2) with four biological replicates. Relevant mock treatments were run in parallel on the same plate for

each mitochondrial inhibitor. To perform gene expression analysis under standard light conditions, the seedlings were kept in the light after transfer to the 96-well plate for 1 h before treatment, and during the treatment (Figure S5). For graphical representation, the relative transcript level of each gene was derived by comparing mock and treated seedlings and setting the 0 h time point to fold change 1.

For gene expression analyses in Col-0 and mutants (listed in the key resources table) 12-day-old seedlings were sprayed with 25 μM antimycin A and Mito-paraquat in water with 0.01% Tween-20 and kept under standard light conditions throughout the treatment time. For gene expression studies in mature plants, four-week-old plants grown in soil pots, were sprayed with 25 μM antimycin A or Mito-PQ in water with 0.01% Tween-20 and left in standard growth conditions (Figure S6). We used *prxII F cyt-roGFP2-Orp1* sensor lines in gene expression analysis (Figures S6 and S7).

RNA extraction, cDNA synthesis, and RT-qPCR

Frozen tissue samples were ground using a Qiagen TissueLyser II and RNA extraction was performed using Spectrum Plant Total RNA Kit (Sigma-Aldrich, STRN250-1KT) with On-Column deoxyribonuclease (DNase) treatment (Sigma-Aldrich, DNASE70) according to the manufacturer's instructions from Sigma. 1 μg of total RNA was used for single stranded cDNA synthesis by using Bio-Rad iScript cDNA Synthesis Kit (Bio-Rad, Hercules, CA, USA). RT-qPCR was performed using diluted cDNA and SYBR green, fluorescent dye (SsoAdvanced Universal Sybr green mix, Bio-Rad). *Arabidopsis* UBIQUITIN-CONJUGATING ENZYME 21 (UBC21) was used as internal control. Primers used in this study are shown in Table S3. RT-qPCR analysis was performed as previously described[116] in a CFX384 Real-time PCR Detection System (Bio-Rad) using the following thermal cycling conditions: 95°C for 2 min, followed by 40 cycles of 95°C for 10 s and 60°C for 10 s. Transcripts were measured in technical duplicates from four independently biological replicates. Statistical analysis was performed using two-way ANOVA with Bonferroni's multiple comparisons test.

Measurements of mitochondrial oxygen consumption rate in isolated mitochondria

Mitochondria were isolated from two-week-old *Arabidopsis* plants grown in liquid half-strength MS medium according to Tran and Van Aken.[117] Briefly, plant material was ground in a pre-cooled mortar with grinding medium (0.3 M sucrose, 25 mM tetrasodium pyrophosphate, 2 mM EDTA, 10 mM KH_2PO_4-HCl, pH 7.5, 1% (w/v) polyvinylpyrrolidone-40 (PVP-40), 1% (w/v) BSA), maintaining a low-temperature environment. The resulting homogenate was filtered through miracloth, with any remaining solid material re-ground and filtered again. Subsequently, the homogenate was transferred into pre-cooled centrifuge tubes, and cellular debris and nuclei were pelleted in the first centrifugation step (5 min at 2500 × *g* at 4 °C). The supernatant was collected and subjected to a second centrifugation at a higher speed (20 min at 17500 × *g* at 4 °C). Following this, the supernatant was removed, and the crude mitochondria pellets were gently resuspended in 1X wash buffer with BSA (0.6 M sucrose, 20 mM TES, 0.2% (w/v) BSA). These centrifugations (low and high) steps were repeated one more time. Further purification of mitochondria was performed by Percoll gradient separation (40 min at 40,000 × *g* at 4 °C), followed by additional washings with 1X wash buffer without BSA. Mitochondrial concentration was determined using Bradford assays.

Oxygen consumption rate was measured in freshly isolated mitochondria using a Clark-type oxygen electrode as described in Lyu et al.[118] In brief, freshly isolated mitochondria (150 μg) were added in 1 mL of respiration buffer (300 mM sucrose, 100 mM NaCl, 5 mM KH_2PO_4, 2 mM MgSO4, 10 mM TES, 0.1% BSA, pH 7.2) to the electrode chamber equipped with a magnetic stir bar. Respiration was initiated by adding substrates (succinate and NADH) along with ADP to simulate ADP-stimulated respiration. The effects of chemicals or inhibitors (according to Table S2) on oxygen consumption rates were determined during the linear phases State III, both in the presence and absence of chemicals. The obtained oxygen consumption rate was subsequently normalized to mitochondrial protein and expressed as oxygen consumption nanomole O_2 per minute per milligram of mitochondrial protein. Statistical analysis was performed using Student's t-test.

Mitochondrial membrane potential measurements

For *in vivo* measurements, 5-to-7-day-old seedling of mito-GFP line were used for mock and chemical treatments (Table S2) in half-strength MS liquid media. The treated seedlings were equilibrated with 20 nM Tetramethylrhodamine Methyl Ester Perchlorate (TMRM) dye (Thermo Fisher) for 20 min prior to imaging. Root epidermal cells were then visualized with a Leica TCS SP8 DLS confocal microscope and a sequential acquisition was performed for GFP (Ex 488/Em 505-530) and TMRM fluorescence (543/565-615). The obtained images were processed in Fiji/ImageJ and presented in the results.[115]

In isolated mitochondria, $\Delta\psi_m$ measurements were performed with safranin O (Sigma-Aldrich), a lipophilic cationic dye that accumulates in mitochondria according to inner membrane potential. The change in absorption and self-quenching under different conditions was continuously monitored in a UV/vis DW2 spectrophotometer (Aminco/Olis, Georgia USA) with dual wavelength (A_{511}-A_{533}, 1 nm slit) according to Moore and Bonner.[119] Briefly, 250-300 μg of freshly isolated mitochondria from wild type *Arabidopsis* were put into a cuvette containing 980 μL assay buffer (0.3 M mannitol, 5 mm $MgCl_2$, and 20 mm Hepes, pH 7.2) supplemented with 10 μM safranin O. Real-time changes in the absorbance of safranin O was monitored during further additions of substrate (NADH) and mitochondrial inhibitors/chemicals, indicated in the figures (Table S2).

Measurements of mitochondrial ROS/H_2O_2 in isolated mitochondria

H_2DCF-DA (2′,7′-Dichlorofluorescein diacetate) based assessment of mtROS/H_2O_2 was performed in freshly isolated mitochondria from *Arabidopsis* according to the method described by Belt et al.[33] Briefly, 10 μg of mitochondria were transferred into black 96-well

Please cite this article in press as: Khan et al., Mitochondria-derived reactive oxygen species are the likely primary trigger of mitochondrial retrograde signaling in *Arabidopsis*, Current Biology (2023), https://doi.org/10.1016/j.cub.2023.12.005

plates in 50 μL of respiration buffer containing 10 μM H_2DCF-DA and incubated for 5 min at room temperature. Chemicals (Table S2) and substrates (5 mM malate + 10 mM glutamate) were diluted in 50 μL of respiration buffer and transferred into the plate to total well volume of 100 μL. These solutions were mixed by shaking inside the plate reader and fluorescence was measured in a BMG Clariostar Plus at 482±10 nm and 530 ±10 nm excitation and emission, respectively, for 60 min with an interval time of 2 min. The slope was calculated from the obtained data using MARS Data Analysis Software.

Mitochondrial H_2O_2 production was measured in isolated mitochondria using Amplex Red (Invitrogen) according to the previously described method.[120] Briefly, 10 μg freshly isolated mitochondria in 50 μL standard respiration buffer supplemented with 100 μM Amplex Red, 2 μL horseradish peroxidase (10 units/mL) and mitochondrial inhibitors /chemicals (Table S2) were loaded on a black 96-well plate. Base line fluorescence of the probe was monitored at 563±10 nm excitation and 570±10 nm emission wavelengths in a BMG Clariostar Plus plate reader for 10 min. After pausing the run, equal volumes of respiration buffer containing substrate (5 mM malate + 10 mM glutamate) was added to the preloaded wells to initiate the reaction. Fluorescence measurements were resumed after the addition and continued for 60 min. The slope was calculated in MARS analysis software. Statistical analysis was performed using one-way ANOVA with Bonferroni's multiple comparisons test.

QUANTIFICATION AND STATISTICAL ANALYSIS

For sensor lines, the acquired fluorescence ratiometric data were logarithmically transformed using a base of 2 (Log_2) and subsequently utilized for statistical comparisons among the chemical treatments throughout the measurement period. To determine the statistical significance, a two-way ANOVA test was employed. Post-hoc tests were performed using Bonferroni correction method for multiple comparisons in GraphPad Prism 8 (GraphPad Software, USA). The first significant difference is denoted by asterisks (*) in the figures. Similarly, Log_2-transformed fold change data derived from RT-qPCR were employed to assess the statistical significance in gene expression differences at different timepoints. Statistical significance levels were indicated as *p <0.05, **p <0.01, ***p <0.001.